

UNIVERSITY OF READING

**Analysis and Computation of Steady Open
Channel Flow using a Singular Perturbation
Problem**

by

I MacDonald, M J Baines and N K Nichols

Numerical Analysis Report 7/94

DEPARTMENT OF MATHEMATICS

**Analysis and Computation of Steady Open
Channel Flow using a Singular Perturbation**

Problem [†]

I MacDonald, M J Baines and N K Nichols

Numerical Analysis Report **7/94**

Department of Mathematics
University of Reading
P O Box 220
Reading
RG6 2AX
United Kingdom

[†]This work forms part of the research programme of the Institute for Computational Fluid Dynamics at Oxford and Reading and was supported by the SERC and HR Wallingford Ltd.

Abstract

In this work we consider steady state solutions of the Saint-Venant equations. We approach these solutions by adding a small artificial viscosity term to the steady Saint-Venant equations and then considering the limit as this term goes to zero. We show that for a uniform rectangular channel, and under certain assumptions, that this limiting process gives a unique physical solution to the problem. We show that in these cases the limiting process also gives us a well-behaved numerical scheme for the computation of this solution. Numerical results are given for a set of test problems and compared with the analytic solutions.

Contents

1	Background	2
2	Regularisation of the Problem	9
3	Numerical Solution of the Regularised Problem	13
4	Results	16
5	Analysis of a Class of Singular Perturbation Problems	23
6	Analysis of a Class of Monotone Difference Schemes for the Singular Perturbation Problem	26
7	Conclusions and Further Work	32
A	Notation	35
B	Details of Test Problems	36

1 Background

1.1 The Steady Saint-Venant Equations

The flow of water in an open channel can be modelled by the Saint-Venant equations. This model approximates the actual flow by a one-dimensional flow. A system of two conservation laws is derived using principles of mass and momentum balance. For these equations to be valid various assumptions about the channel and the flow are required, but we will not consider the question of validity here. A derivation of the Saint-Venant equations can be found in Cunge *et al*[3].

In this work we investigate steady state solutions of the Saint-Venant equations and in particular numerical methods for their computation. By steady state solutions we mean solutions that are constant in time. We are interested in such solutions from a practical point of view since steady flow often occurs in nature.

A steady form of the Saint-Venant equations, which we refer to as the steady Saint-Venant equation, is found by assuming that all the variables are time invariant in the unsteady equations. We state the steady Saint-Venant equation below.

Let the x -axis be horizontal and in a direction along the channel length. Figure 1 shows a typical channel cross-section normal to the x -axis. Let $y(x)$ be the depth of the flow at this section, which is the height of the free surface (assumed to be a horizontal line) above the lowest point in the section, and $Q(x)$ be the discharge, the rate at which a volume of water flows through the section. We also need the following functions which come from the shape of the section:
 $\sigma(x, \eta)$: Width of the section at height η above the lowest point in the section.

$A(x, y)$: Cross-sectional area of the flow passing through the section, for depth y , and given by

$$A(x, y) = \int_0^y \sigma(x, \eta) d\eta. \quad (1.1)$$

$P(x, y)$: Perimeter length of the flow in contact with the channel.

Figure 2 shows a side view of the channel with the channel bottom a distance $z(x)$ below the x -axis. Let $S_0(x) = \frac{dz}{dx}$ be the slope of the channel bed. The height of the free surface above the x -axis is given by $y(x) - z(x)$.

The steady form of the conservation of mass equation is then

$$Q(x_1) = Q(x_2), \quad (1.2)$$

for any x_1, x_2 along the channel. This equation is trivial and tells us that the discharge is constant throughout the length of the channel. In future we will take this constant value as a known parameter Q .

The corresponding “conservation of momentum” equation is

$$F(x_2, y(x_2)) - F(x_1, y(x_1)) = \int_{x_1}^{x_2} d(x, y(x)) dx, \quad (1.3)$$

for any x_1, x_2 along the channel. Here F is a quantity called the Specific Force given by

$$F(x, y) = \frac{Q^2}{A(x, y)} + g \int_0^y (y - \eta) \sigma(x, \eta) d\eta, \quad (1.4)$$

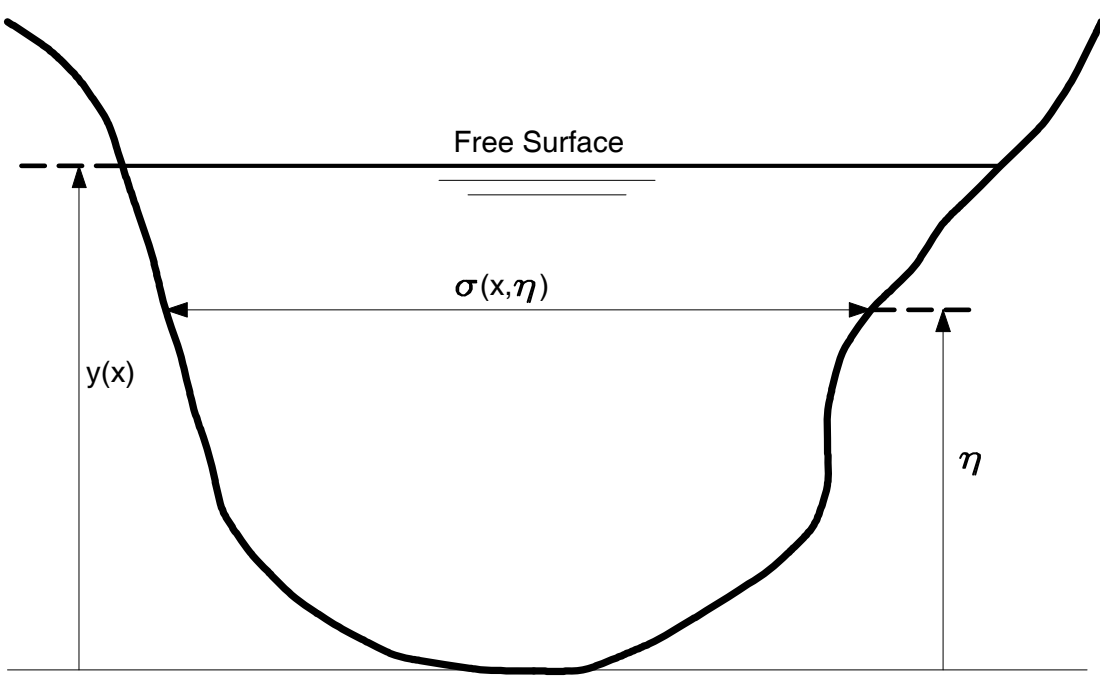


Figure 1: Cross-section of channel, normal to x -axis

where g is the acceleration due to gravity. This quantity has units of force per unit mass and has two components. The first term is the momentum flux due to the flow of water and the second is due to hydrostatic pressure forces. The source term $d(x, y)$ is given by

$$d(x, y) = gA(x, y) (S_0(x) - S_f(x, y)) + g \int_0^y (y - \eta) \frac{\partial}{\partial x} \sigma(x, \eta) d\eta. \quad (1.5)$$

The friction slope, S_f , models the effects of channel friction and turbulence. There are several common forms for this term; we shall use the form due to Manning (see Chow [2]), which is given by

$$S_f(x, y) = Q|Q|n^2 \frac{[P(x, y)]^{4/3}}{[A(x, y)]^{10/3}}, \quad (1.6)$$

where n is the Manning roughness coefficient which controls the roughness of the channel.

From now on we shall make the assumption that $Q > 0$ without loss of generality, since if $Q < 0$ we can simply reverse the x -direction. Also the case $Q = 0$ is trivial.

At any point along the channel where the depth y behaves smoothly, and as long as the channel geometry is smooth enough, we can take the limit as $x_1 \rightarrow x_2 \rightarrow x$ in equation (1.3) to obtain the differential equation

$$\frac{d}{dx} F(x, y) = d(x, y). \quad (1.7)$$

It is clear that if a stretch of channel has a discontinuous flow then this differential equation does not describe the flow globally. The integral form (equation 1.3),

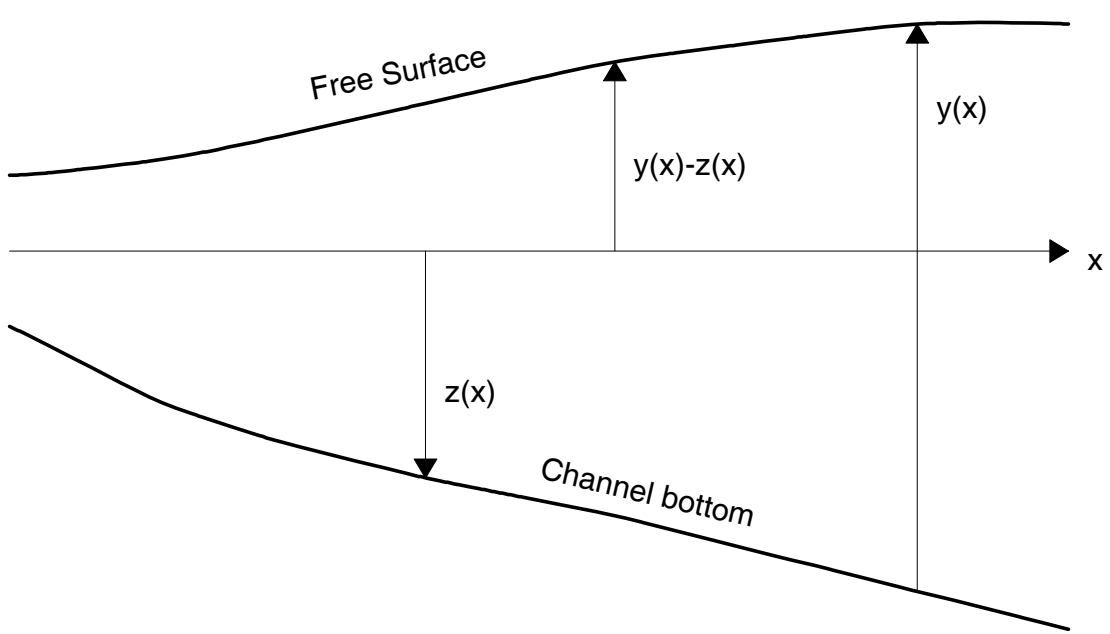


Figure 2: Side view of channel

however, allows discontinuities, namely hydraulic jumps. From (1.3) any hydraulic jump must satisfy the jump condition

$$F(x^*, y_L) = F(x^*, y_R), \quad (1.8)$$

where $x = x^*$ is the position of the jump and y_L, y_R are the depths on the left and right of the jump respectively. Combining the differential equation (1.7) and the jump condition (1.8), we can construct a family of general solutions to the integral form (1.3), although, not all of these solutions will be physically allowed. The unphysical solutions are those where the flow gains energy across a hydraulic jump rather than dissipating energy. This is not allowed because it violates a fundamental law of thermodynamics.

The most common form of equation (1.7) is with the left-hand side differentiated out to give a differential equation in standard form

$$\frac{dy}{dx} = \frac{\Gamma_1(x, y)}{\Gamma_2(x, y)}, \quad (1.9)$$

where

$$\Gamma_1(x, y) = S_0(x) - S_f(x, y) + \frac{Q^2}{g[A(x, y)]^3} \int_0^y \frac{\partial}{\partial x} \sigma(x, \eta) d\eta,$$

and

$$\Gamma_2(x, y) = 1 - [F_r(x, y)]^2.$$

The Froude Number, F_r , given by

$$F_r(x, y) = \sqrt{\frac{Q^2 \sigma(x, y)}{g[A(x, y)]^3}}, \quad (1.10)$$

is an important parameter, because it indicates the state of the flow at a given section for a given discharge and depth. For $F_r < 1$ gravitational forces dominate

inertial forces and the flow is said to be subcritical. For $F_r > 1$ the inertial forces dominate gravitational forces and the flow is said to be supercritical. The behaviour for these two types of flow is significantly different. For $F_r = 1$ the flow is said to be critical. Note that $\Gamma_2 \rightarrow 0$ as $F_r \rightarrow 1$, so that $|\frac{dy}{dx}|$ becomes unbounded as the flow approaches criticality. Because of the assumptions about the smoothness of the flow the differential equation will break down at this point.

1.2 Solution Profiles for a Rectangular Channel

Although the solutions to equation (1.9) for a general channel shape are difficult to obtain, for certain channel geometries we can get a very good idea of how the solutions behave. Suppose that we restrict attention to a uniform rectangular channel given by $\sigma(x, \eta) = B$, $A(x, y) = By$, $P(x, y) = 2y + B$, where $B > 0$ is a constant. We will also assume that the bed slope, S_0 , is constant. Equation (1.9) then becomes the autonomous equation

$$\frac{dy}{dx} = \frac{\Gamma_1(y)}{\Gamma_2(y)}, \quad (1.11)$$

where

$$\Gamma_1(y) = S_0 - Q^2 n^2 \frac{(2y + B)^{4/3}}{(By)^{10/3}},$$

and

$$\Gamma_2(y) = 1 - \left(\frac{y_c}{y}\right)^3.$$

Here

$$y_c = \sqrt[3]{\frac{Q^2}{gB^2}},$$

is the critical depth. For $y < y_c$ the flow is supercritical and we have $\Gamma_2 < 0$. For $y > y_c$ the flow is subcritical and we have $\Gamma_2 > 0$.

For $S_0 > 0$ we can also find a unique root, y_n , to $\Gamma_1 = 0$. This depth is called the normal depth. We also have that $\Gamma_1 < 0$ for $y < y_n$ and $\Gamma_1 > 0$ for $y > y_n$. For the case $S_0 \leq 0$ we have $\Gamma_1 < 0$ for all y . In this case the normal depth strictly doesn't exist, but for convenience it can be given a value of $+\infty$. The following properties of Γ_1/Γ_2 are then easy to show:

$$\left| \frac{\Gamma_1}{\Gamma_2} \right| \rightarrow \infty, \quad \text{as } y \rightarrow y_c, \quad \text{provided } y_n \neq y_c. \quad (1.12)$$

$$\left| \frac{\Gamma_1}{\Gamma_2} \right| \rightarrow 0, \quad \text{as } y \rightarrow y_n, \quad \text{provided } y_n \neq y_c. \quad (1.13)$$

$$\frac{\Gamma_1}{\Gamma_2} \rightarrow S_0, \quad \text{as } y \rightarrow \infty. \quad (1.14)$$

Equation (1.14) implies that for large y the free surface becomes horizontal, since the distance of the free surface above the x -axis is given by $y(x) - z(x)$ and

$$\frac{d}{dx}(y(x) - z(x)) = \frac{\Gamma_1}{\Gamma_2} - S_0 \rightarrow 0 \quad \text{as } y \rightarrow \infty.$$

For any y we can also obtain the sign of Γ_1/Γ_2 and hence decide whether the depth is increasing or decreasing. To do this we divide the positive y -axis into three regions as follows:

Region	y interval	Sign of Γ_1/Γ_2
1	$y > \max\{y_n, y_c\}$	+
2	$\min\{y_n, y_c\} < y < \max\{y_n, y_c\}$	-
3	$0 < y < \min\{y_n, y_c\}$	+

Note that for $S_0 \leq 0$, region 1 doesn't exist since $y_n = +\infty$.

The main question now is how do we determine the relative positions of y_n and y_c ? It turns out that this can be done by classifying the slope, S_0 , as follows (see Chow[2]). Let us define the critical slope S_{0c} by

$$S_{0c} = Q^2 n^2 \frac{(2y_c + B)^{4/3}}{(By_c)^{10/3}} > 0,$$

then

$$\begin{aligned} S_0 \leq 0 &\implies \text{ADVERSE SLOPE} && \text{and } y_n = +\infty, \\ 0 < S_0 < S_{0c} &\implies \text{MILD SLOPE} && \text{and } y_n > y_c, \\ S_0 = S_{0c} &\implies \text{CRITICAL SLOPE} && \text{and } y_n = y_c, \\ S_0 > S_{0c} &\implies \text{STEEP SLOPE} && \text{and } y_n < y_c. \end{aligned}$$

Now, using all the previous information we can determine the behaviour of the solution for each region and for each different slope. Figures 3, 4 and 5 show how the solutions behave for mild, steep and adverse slopes. We label each of the possible types of flow profile by an expression such as $S2$, where S stands for steep slope and 2 stands for region 2.

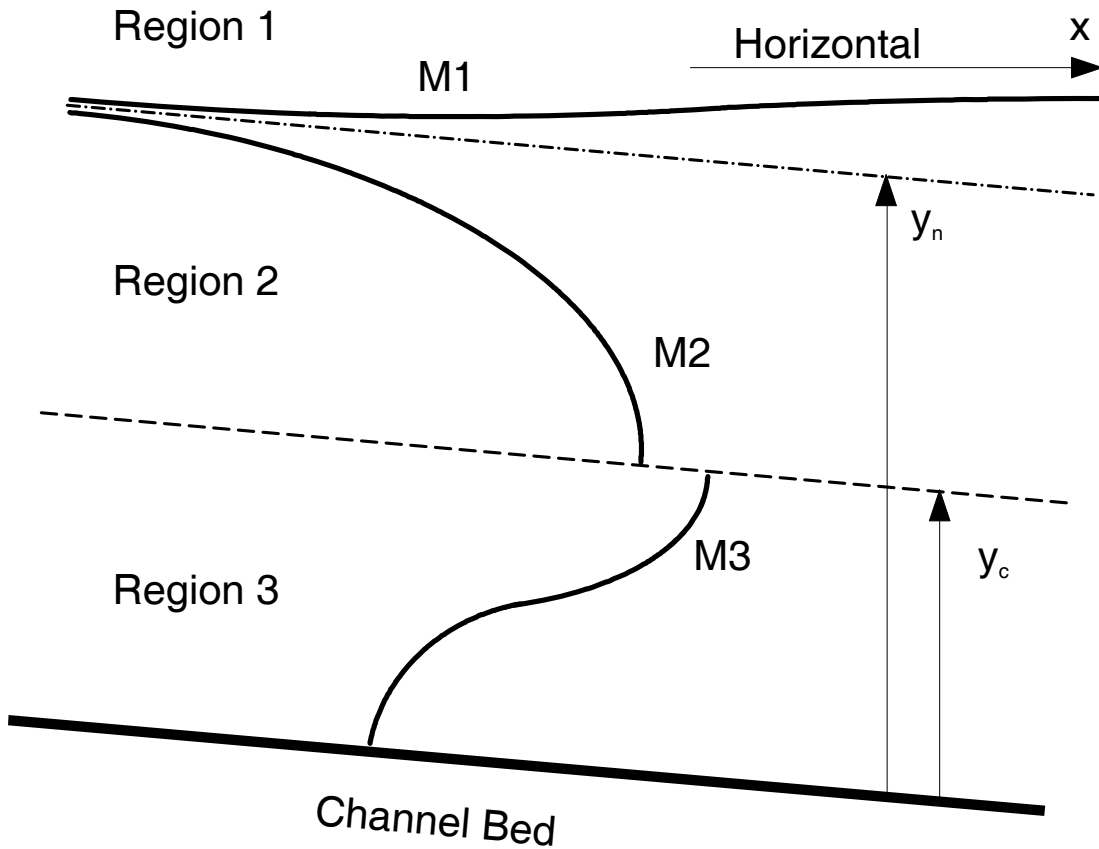


Figure 3: Flow profiles for a mild channel

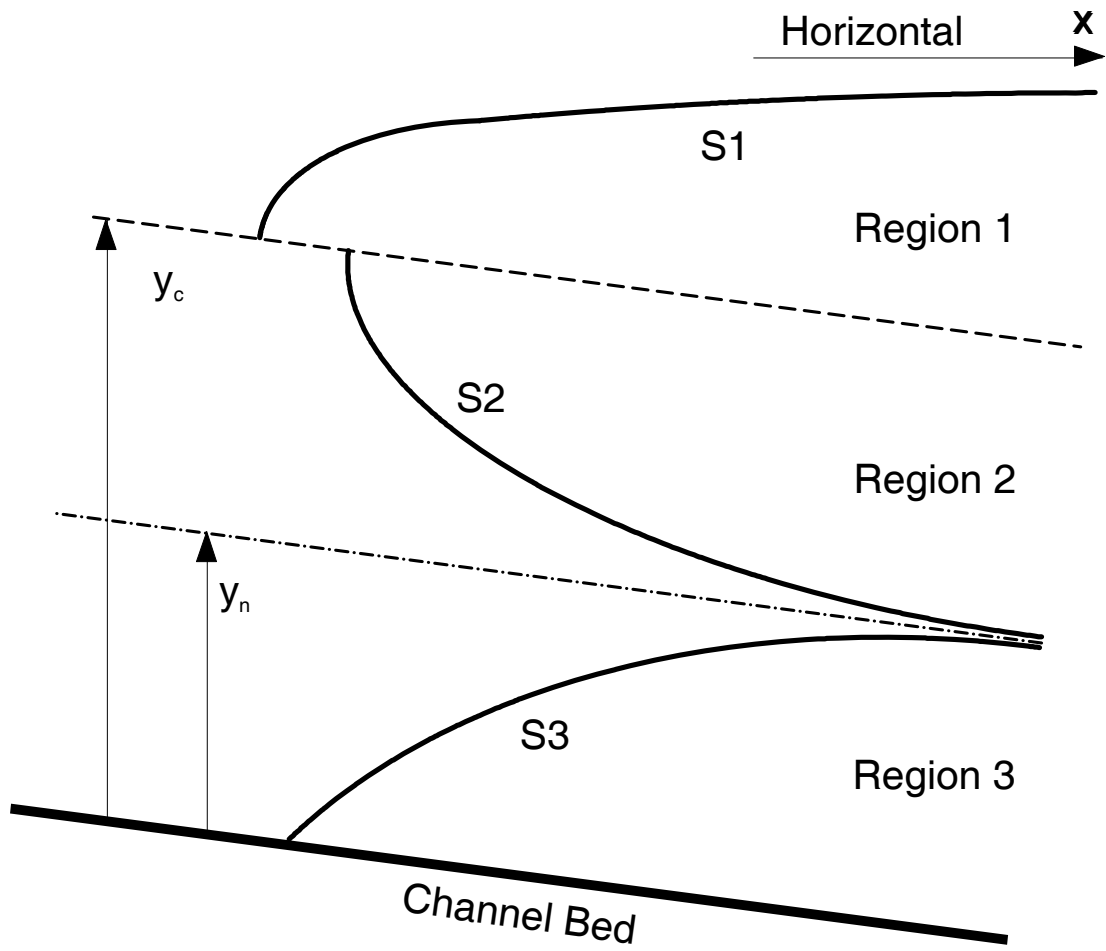


Figure 4: Flow profiles for a steep channel

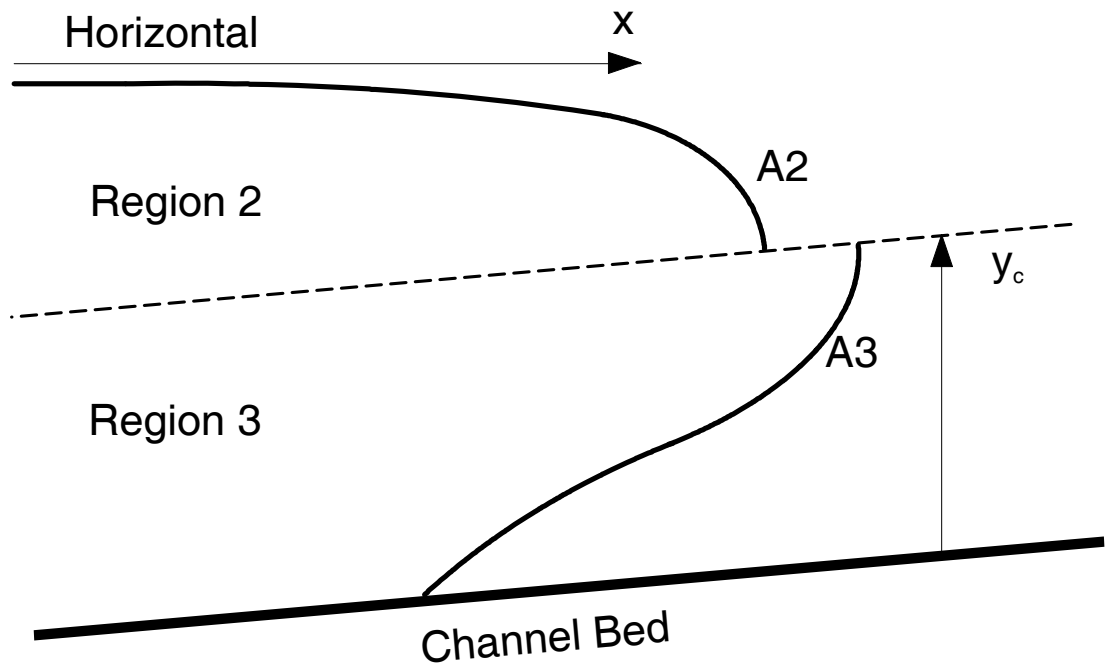


Figure 5: Flow profiles for an adverse channel

2 Regularisation of the Problem

Suppose that we have a stretch of channel in the interval $[0, L]$ where $L > 0$. A steady solution of the Saint-Venant equations in this channel is given by a function y that satisfies

$$F(x_2, y(x_2)) - F(x_1, y(x_1)) = \int_{x_1}^{x_2} d(x, y(x)) dx, \quad (2.15)$$

for any $x_1, x_2 \in [0, L]$. We may also require the depth to have certain values at the boundaries. It is much easier to work with the interval $[0, 1]$ so we put $\tilde{x} = x/L$ and $\tilde{y}(\tilde{x}) = y(x)$ to arrive at

$$F(\tilde{x}_2 L, \tilde{y}(\tilde{x}_2)) - F(\tilde{x}_1 L, \tilde{y}(\tilde{x}_1)) = L \int_{\tilde{x}_1}^{\tilde{x}_2} d(\tilde{x} L, \tilde{y}(\tilde{x})) d\tilde{x}, \quad (2.16)$$

for any $\tilde{x}_1, \tilde{x}_2 \in [0, 1]$. Where \tilde{y} is smooth it satisfies the differential equation

$$\frac{d}{d\tilde{x}} F(\tilde{x} L, \tilde{y}(\tilde{x})) = L d(\tilde{x} L, \tilde{y}(\tilde{x})). \quad (2.17)$$

In future we will drop the tildes.

A common technique for analysing problems with solutions that may be discontinuous is to study a family of problems having smooth solutions with these solutions tending to the discontinuous solution of the original problem in some limit. In this work we proceed in a similar manner as that for first order conservation laws such as the Inviscid Burger's equation (see LeVeque[7]). We add a small artificial viscosity term to equation (2.17) in the expectation that this will ensure the existence of smooth solutions to the resulting problem. We then look at the limit of these smooth solutions as the "viscosity" tends to zero.

The family of problems that we shall study is generated by varying the viscosity ϵ in the problem

$$\epsilon \frac{d^2 y}{dx^2} - \frac{d}{dx} f(x, y) - b(x, y) = 0, \quad 0 \leq x \leq 1, \quad y > 0, \quad (2.18)$$

$y(0) = \gamma_0$, $y(1) = \gamma_1$, where $\epsilon, \gamma_0, \gamma_1 > 0$. Here $f(x, y) = -F(xL, y)$ and $b(x, y) = Ld(xL, y)$. Clearly for $\epsilon \rightarrow 0$, we recover equation (2.17). We denote problem (2.18) by P_ϵ and its solution by y_ϵ (if it exists).

P_ϵ is a two point boundary value problem and hence always requires boundary conditions at both ends of the channel, whereas the original problem can have none, one or two boundary conditions. Because of this feature we may need to supply artificial boundary values for P_ϵ , which we shall usually take as the critical depth.

Solutions to singular perturbation problems, such as P_ϵ , have certain well known features (see Ascher *et al*[1], O'Malley[12], Pearson[15]). In the interior of the domain we find transition layers, i.e. regions where the solution changes extremely rapidly. The region in which these rapid changes occur gets narrower as ϵ gets smaller and we expect the transition layer to tend to a discontinuity as ϵ tends to zero. An important question is whether in the limit, these discontinuities satisfy the jump condition (1.8). The regions of sharp variation can also occur

at the boundaries, in which case they are called boundary layers. In the limit we expect these layers to tend to a discontinuity at the boundary and in particular expect them to occur when invalid or artificial values are given as boundary data. By this mechanism we also expect the flow in the interior of the domain to be able to disregard any artificial or invalid boundary values if necessary.

The above discussion is just speculation at this stage; we require some very important questions to be asked, most of which we cannot answer for a general channel. The questions are as follows:

1. Does P_ϵ have a unique solution for ϵ in some range, where ϵ can get arbitrarily close to zero?
2. Can we construct a convergent sequence $\{y_{\epsilon_n}\}$ of such solutions, with $\epsilon_n \rightarrow 0$ as $n \rightarrow \infty$?
3. Does the limit of this sequence of solutions satisfy equation (2.16)?
4. Is this limit solution always physically allowable?

We now proceed to give answers to these questions in a special, but useful case. The proofs of the theorems required are postponed to section 5 and only quoted here. We consider a uniform rectangular channel where the bed slope is strictly positive. The exact assumptions are as follows:

$$\left. \begin{aligned} \sigma(x, y) &= B = \text{constant}, \\ A(x, y) &= By, \\ P(x, y) &= 2y + B, \\ L, Q, B, n &> 0, \\ S_0 &\in C^1[0, L], \\ S_0(x) &> 0 \quad \forall x \in [0, L]. \end{aligned} \right\} \quad (2.19)$$

The resulting functions f and b are given by

$$f(x, y) = f(y) = -\frac{Q^2}{By} - \frac{1}{2}gBy^2, \quad (2.20)$$

$$b(x, y) = gBLy \left[S_0(xL) - \left(\frac{Qn}{By} \right)^2 \left(\frac{2}{B} + \frac{1}{y} \right)^{4/3} \right]. \quad (2.21)$$

It is easily seen that under the assumptions given, we have $b_x, b_y, b_{xy} \in C^0([0, 1] \times (0, \infty))$, $f \in C^2(0, \infty)$ and

$$b_y(x, y) = gBLS_0(xL) + gL \left(\frac{Qn}{By} \right)^2 \left(\frac{2}{B} + \frac{1}{y} \right)^{1/3} \left(2 + \frac{7B}{3y} \right), \quad (2.22)$$

is strictly positive. We also observe that

$$b(x, y) \rightarrow +\infty, \quad \text{as } y \rightarrow \infty, \quad (2.23)$$

$$b(x, y) \rightarrow -\infty, \quad \text{as } y \rightarrow 0, \quad (2.24)$$

and since b_y is always positive it is clear that, for any $x \in [0, 1]$, there is a unique depth $y_n(x)$ such that $b(x, y_n(x)) = 0$. This depth is the normal depth mentioned

in the previous section, but, since the channel slope now varies with x , the normal depth also varies with x . It is easy to show that the function $y_n(x)$ is bounded, so let $M = \max\{y_n(x) : x \in [0, 1]\}$ and $m = \min\{y_n(x) : x \in [0, 1]\}$; hence

$$\begin{aligned} (x, y) \in [0, 1] \times (0, m] &\implies b(x, y) \leq 0, \\ (x, y) \in [0, 1] \times [M, \infty) &\implies b(x, y) \geq 0. \end{aligned} \tag{2.25}$$

Under the above assumptions about the channel we can apply theorem 1 of section 5. This proves that P_ϵ has a unique solution, $y_\epsilon \in C^2[0, 1]$, for all $\epsilon > 0$. The theorem also gives the bound

$$\min\{\gamma_0, \gamma_1, m\} \leq y_\epsilon(x) \leq \max\{\gamma_0, \gamma_1, M\}, \quad 0 \leq x \leq 1. \tag{2.26}$$

The next question to be answered is what happens when we let ϵ tend to zero. Theorem 2 of section 5 shows that, given a sequence $\{\epsilon_n\}$ with $\epsilon_n > 0$ and $\epsilon_n \rightarrow 0$ as $n \rightarrow \infty$, then there is a subsequence $\{\epsilon_{n_k}\}$ such that

$$y_{\epsilon_{n_k}} \rightarrow Y \in NBV \quad \text{a.e. as } k \rightarrow \infty. \tag{2.27}$$

Let the set NBV be the set of all functions u of finite variation such that for $x \in [0, 1)$

$$u(x) = u(x+) = \lim_{\delta \downarrow x} u(\delta) \tag{2.28}$$

and

$$u(1) = u(1-) = \lim_{\delta \uparrow 1} u(\delta). \tag{2.29}$$

It is a property of functions of finite variation that these limits always exist.

Next we ask whether the limit function Y has the desired properties. In particular, we would like it to be the physical solution of (2.16). Theorems 3 and 5 of section 5 show that Y satisfies the reduced differential equation (2.17) in intervals where it is continuous. Also we show in section 5 that at discontinuities the jump conditions (1.8) are satisfied. These two facts are enough to ensure that Y satisfies the integral relation (2.16).

For a rectangular channel, only hydraulic jumps from supercritical to subcritical flow are physically allowed due to energy considerations. It can easily be seen that, since f is strictly concave and maximum at the critical depth, condition (ii) of theorem 5 of section 5 tells us that Y can only have such physical jumps.

Although we have shown that the limit function Y is a physical solution of the integral relation (2.16) we require more for Y to be useful. We need to have some control over Y , i.e. be able to specify the depths at the channel ends. We can apparently do this by assigning γ_0, γ_1 appropriate values, but the situation is more complicated than it seems. First we discuss what boundary conditions we may apply to the steady flow problem (see Chow [2]). At $x = 0$ we can only assert that the depth has a certain value if this value is supercritical. If no condition is given at this point a subcritical depth occurs at the boundary. At $x = 1$ we can only assert that the depth has a certain value if this value is subcritical. If no condition is given at this point a supercritical depth occurs at the boundary. The difficulty arises for the following reason: Given an arbitrary set of valid boundary conditions (as described above) which may be at both ends

or just on end, then there does not always exist a solution satisfying the full set of boundary conditions and it is often impossible to tell in advance when this is the case. There will always be flows satisfying subsets (which may be empty) of the boundary conditions, and it is of use to us to find the “strongest” of these flows (in the sense of greatest Specific Force throughout the channel). This “strongest” flow will always satisfy the maximum possible number of boundary conditions and will tell us which of the given boundary conditions are too weak, if any, by overriding them.

We choose γ_0 and γ_1 by giving them the values of the corresponding valid boundary condition if there is one, or else the critical depth is assigned. Condition (iii) of theorem 5 gives us some information about how the given values of γ_0 and γ_1 influence Y at the boundaries. It is easy to show that the following implications hold:

$$\begin{aligned}
 \gamma_0 \geq y_c &\implies Y(0) \geq y_c, \\
 \gamma_0 \leq y_c &\implies Y(0) = \gamma_0 \text{ or } Y(0) \geq \gamma_0^* \geq y_c, \\
 \gamma_1 \leq y_c &\implies Y(1) \leq y_c, \\
 \gamma_1 \geq y_c &\implies Y(1) = \gamma_1 \text{ or } Y(1) \leq \gamma_1^* \leq y_c.
 \end{aligned}
 \tag{2.30}$$

The star superscript denotes the corresponding sequent depth, i.e. y^* is the depth such that $f(y) = f(y^*)$ and $(y - y_c)(y^* - y_c) \leq 0$. From (2.30) it can be shown that Y depends on γ_0, γ_1 in the way we require. Y satisfies any valid boundary conditions if possible and if this is not possible then Y overrides the boundary conditions as described previously.

From the above discussion it appears that in the case considered we can use the limit of solutions of P_ϵ to define, for a particular set of boundary conditions, the unique physical solution, $Y \in NBV$, of the integral relation (2.16). The uniqueness can be argued from theorem 4 of section 5.

3 Numerical Solution of the Regularised Problem

In this section we look at a numerical scheme for solving the singular perturbation problem (2.18). As in section 2 the theory that we shall give only applies to channels satisfying assumptions (2.19), although the scheme can be applied under less restrictive conditions. In section 6 we include some analysis for a class of monotone schemes. However, here we shall just discuss one case, which is the scheme due to Engquist and Osher[4][5]. We choose this scheme since it has been successfully used for similar singular perturbation problems before (see Osher[13][14] and Glaister[6]). In this work we use a uniform grid, $x_i = ih$, $i = 0, 1, \dots, N$, of spacing $h = 1/N$, where $N - 1 \in \mathbb{N}$. The difference scheme can be written as follows:

$$\frac{\epsilon}{h^2} (u_{i+1} - 2u_i + u_{i-1}) - \frac{1}{h} (f_-(u_{i+1}) - f_-(u_i) + f_+(u_i) - f_+(u_{i-1})) - b(x_i, u_i) = 0, \quad (3.31)$$

$i = 1, \dots, N - 1$, with

$$u_0 = \gamma_0, \quad u_N = \gamma_1,$$

where, since f is concave we define

$$\begin{aligned} f_+(y) &= f(\min\{y, y_c\}), \\ f_-(y) &= f(\max\{y, y_c\}). \end{aligned} \quad (3.32)$$

Theorem 1 of section 6 shows that this scheme has a unique solution, $\mathbf{u}_h^\epsilon = [u_0^{\epsilon,h}, u_1^{\epsilon,h}, \dots, u_{N-1}^{\epsilon,h}, u_N^{\epsilon,h}]^T$ for all $\epsilon \geq 0$ and all $h = 1/N$, where $N - 1 \in \mathbb{N}$. Moreover, the solution satisfies the bound

$$\min\{\gamma_0, \gamma_1, m\} \leq \mathbf{u}_h^\epsilon \leq \max\{\gamma_0, \gamma_1, M\}, \quad (3.33)$$

where m, M are defined in (2.25). This is an identical bound to that satisfied by the solution of the continuous problem and ensures stability. Using a technique given in Nijima [11] we can also show that the total variation of the numerical solution is uniformly bounded in ϵ and h .

Although this numerical scheme can be used to compute the solution to the singular perturbation problem for any $\epsilon > 0$, in this work we are solely interested in computing the solution of the reduced problem ($\epsilon \rightarrow 0$). Theorem 8 of section 6 gives us a useful result. Suppose we have a sequence of grids with $h_n \rightarrow 0$ as $n \rightarrow \infty$. If U^h is the piecewise constant extension to \mathbf{u}_h^0 , then there exists a subsequence $\{h_{n_k}\}$ such that

$$U^{h_{n_k}} \rightarrow Y \in NBV \quad \text{a.e. as } k \rightarrow \infty. \quad (3.34)$$

Y is the limit function given in section 2 and is the physical solution we require.

Because of the above we see that to approximate the solution of the reduced problem ($\epsilon = 0$) in practice, we do not need to carry out the limiting process, but simply solve the scheme (3.31) with ϵ set to zero.

3.1 Solution of Discrete Equations

Now that we know that the numerical scheme converges as we refine the grid, we need to think about how we calculate the solution of the numerical scheme. This involves solving a system of $N - 1$ nonlinear equations. The most robust method is a pseudo time iteration. Theorem 7 in section 6 gives us the following practical method.

Let $\mathbf{u}^0 = [u_0^0, u_1^0, \dots, u_N^0]^T > 0$, with $u_0^0 = \gamma_1$, $u_N^0 = \gamma_0$ and define $\underline{u} = \min\{m, u_0^0, u_1^0, \dots, u_N^0\}$ and $\bar{u} = \max\{M, u_0^0, u_1^0, \dots, u_N^0\}$, where m, M are given by (2.25). Let $\overline{S_0} = \max\{S_0(x) : x \in [0, 1]\}$, $\underline{S_0} = \min\{S_0(x) : x \in [0, 1]\}$,

$$\overline{b_y} = gLB\overline{S_0} + gL \left(\frac{Qn}{B\underline{u}} \right)^2 \left(\frac{2}{B} + \frac{1}{\underline{u}} \right)^{1/3} \left(2 + \frac{7B}{3\underline{u}} \right), \quad (3.35)$$

and

$$\delta = gLB\underline{S_0} + gL \left(\frac{Qn}{B\bar{u}} \right)^2 \left(\frac{2}{B} + \frac{1}{\bar{u}} \right)^{1/3} \left(2 + \frac{7B}{3\bar{u}} \right). \quad (3.36)$$

If Δt satisfies

$$0 < \Delta t < \left[\frac{2\epsilon}{h^2} + \frac{2}{h} \max\{|f'(\underline{u})|, |f'(\bar{u})|\} + \overline{b_y} \right]^{-1}, \quad (3.37)$$

then the sequence of vectors, $\{\mathbf{u}^n\}_{n=1}^\infty$, given by

$$\begin{aligned} u_i^{n+1} &= u_i^n + \Delta t (T\mathbf{u}^n)_i, \quad i = 1, \dots, N-1, \\ u_0^n &= \gamma_0, \quad u_N^n = \gamma_1, \end{aligned} \quad (3.38)$$

where

$$\begin{aligned} (T\mathbf{u}^n)_i &= \frac{\epsilon}{h^2} (u_{i+1}^n - 2u_i^n + u_{i-1}^n) \\ &\quad - \frac{1}{h} (f_-(u_{i+1}^n) - f_-(u_i^n) + f_+(u_i^n) - f_+(u_{i-1}^n)) - b(x_i, u_i^n), \end{aligned} \quad (3.39)$$

converges to \mathbf{u}_h^ϵ , the solution of (3.31). We also have that

$$\|\mathbf{u}^n - \mathbf{u}_h^\epsilon\|_1 \leq \exp(-n\Delta t\delta) \|\mathbf{u}^0 - \mathbf{u}_h^\epsilon\|_1, \quad (3.40)$$

where $0 < \Delta t\delta < 1$.

Although the above method has the advantage that it is guaranteed to converge, it is also true that, because of the CFL-like condition on Δt , the speed of convergence can be prohibitive. In practice it is more efficient to use Newton's method to solve the nonlinear equations. The speed improvement is very significant since the Jacobian is tridiagonal and hence efficient to invert. Newton's method needs to be modified slightly to prevent solution values from becoming negative. The main drawback of Newton's method is that the initial guess is required to be sufficiently close to the solution for convergence to occur, but we can arrange this by performing some iterations of the time stepping algorithm, before switching to the Newton iteration.

3.2 Post-Processing Solution at Channel Ends

In certain circumstances when invalid or artificial boundary values γ_0, γ_1 are given to the singular perturbation problem, we find that $Y(0) \neq \gamma_0$ and or $Y(1) \neq \gamma_1$, where Y is the solution of the physical solution of the reduced problem. It is the values of $Y(0)$ and $Y(1)$ that we are interested in. If we let $h \rightarrow 0$ we would expect discontinuities in the numerical solution at the boundaries, but a problem arises since we can only solve for finite h , and this results in these discontinuities being smeared under certain conditions. Because of this smearing the numerical solution may not approximate the values of $Y(0)$ and $Y(1)$ very well at grid points close to the ends.

One method to remedy this problem is to post-process the numerical solution near the ends of the channel. The method used here is as follows. If smearing is detected at an end, we artificially extend the channel at that end by a number of grid points (say two) and then re-apply the numerical scheme at that end for a number of grid-points (say five), with an extended boundary condition of y_c . By doing this we find that any smearing is now in the extended region, and that the value at the real boundary is correct. For example, suppose we detect smearing near the boundary $x = 0$, then typically we would add grid points $x_{-1} = -h, x_{-2} = -2h$. We would then apply our numerical scheme to the subgrid $\{x_{-2}, x_{-1}, x_0, x_1, x_2\}$ to solve for $\{w_{-2}, w_{-1}, w_0, w_1, w_2\}$, where we have set boundary conditions $w_{-2} = y_c$ and $w_2 = u_2$. Here u_2 is the value of our original solution vector at x_2 . We now replace elements u_0, u_1 of our original solution vector by w_0 and w_1 respectively. This fix is rather ad hoc, and it is hoped that a more elegant method can be found.

4 Results

In this section we include numerical results from five different test problems. For each test problem the analytic solution is known so we can get a good measure of the performance of the numerical scheme. The test problems were created using an “inverse” approach and are published in MacDonald[10]. Full details of the test problems are given in appendix A. The numerical scheme used is that of Engquist-Osher, as described in the previous section, and all the test problems satisfy assumptions (2.19) so all the theory given in the previous two sections is applicable.

For each test problem we show the exact solution, Y , as well as numerical solutions on various grids. The numerical solution is shown by crosses for $N = 10$, triangles for $N = 25$, circles for $N = 50$ and squares for $N = 100$. For each test problem we also show the channel bed profile, the exact free surface profile, and computed free surface profiles.

4.1 Discussion of Results

The solution to test problem 1 is a smooth subcritical flow. Figure 6 shows the exact solution as well as numerical solutions for $N = 10, 25, 50$. The flow for this problem is controlled by the boundary condition at $x = 100$, so it is not surprising that the numerical errors grow as the solution moves away from this boundary. However, they unexpectedly decrease as the solution approaches the other boundary. It can be seen that the numerical solutions give a good approximation to the exact solution and also it can be seen visually that the accuracy increases as the grid is refined. This has been confirmed experimentally by calculating the L_2 errors for a large range of grids and as expected the scheme is found to give a first order accuracy.

The solution to test problem 2 is a smooth supercritical flow. Figure 8 shows the exact solution as well as numerical solutions for $N = 10, 25$. The flow for this problem is controlled by the boundary condition at $x = 0$, and the numerical errors grow as the solution moves away from this boundary; moreover, as in the previous problem they eventually start to decrease. Again it can be seen that the numerical solutions give a good approximation to the exact solution and also the accuracy increases as we refine the grid.

The solution to test problem 3 is a smooth flow that is subcritical for $x \leq 50$ and supercritical for $x \geq 50$. Figure 10 shows the exact solution as well as numerical solutions for $N = 10, 25$. This problem has no boundary conditions; the flow is controlled by the critical section at $x = 50$. This explains why the numerical errors grow as we move away from this point. Again the numerical solutions give a good approximation to the exact solution and the accuracy increases as we refine the grid.

The solution to test problem 4 is a discontinuous flow with a jump at $x = 200/3$. Figure 12 shows the exact solution as well as numerical solutions for $N = 25, 50, 100$. For this problem a boundary condition is given at $x = 100$. The numerical solutions for this rather hard problem are very good. The jump is resolved very well taking into account the coarseness of the grids used. It can be seen visually that both the position and height of the jumps become more

accurate as the grid is refined, but unlike the previous problems with smooth solutions, there are no simple methods to quantitatively confirm this improvement in accuracy. Further refinement beyond that shown here continues the improvement in the numerical solution.

The solution to test problem 5 is also a discontinuous flow and has a jump at $x = 100/3$. Figure 14 shows the exact solution as well as numerical solutions for $N = 10, 25, 50$. For this problem a boundary condition is given at $x = 0$. Again, taking into account the coarseness of the grids used the scheme is very successful. For example, using only ten grid points, all the important features of the solution are present and we have a good estimate for the position of the jump. This estimate could be used if we wished to refine the grid locally in the neighbourhood of the jump. Again we see that accuracy of both the position and height of the jump increases as the grid is refined. Further refinement than that shown here continues this process.

It is clear that the method proposed here is a very powerful in generating approximate solutions to a range of test problems. We have also carried out numerical experiments on test problems which do not satisfy assumptions (2.19). Although the theoretical results do not hold for these test problems, good numerical results have been obtained.

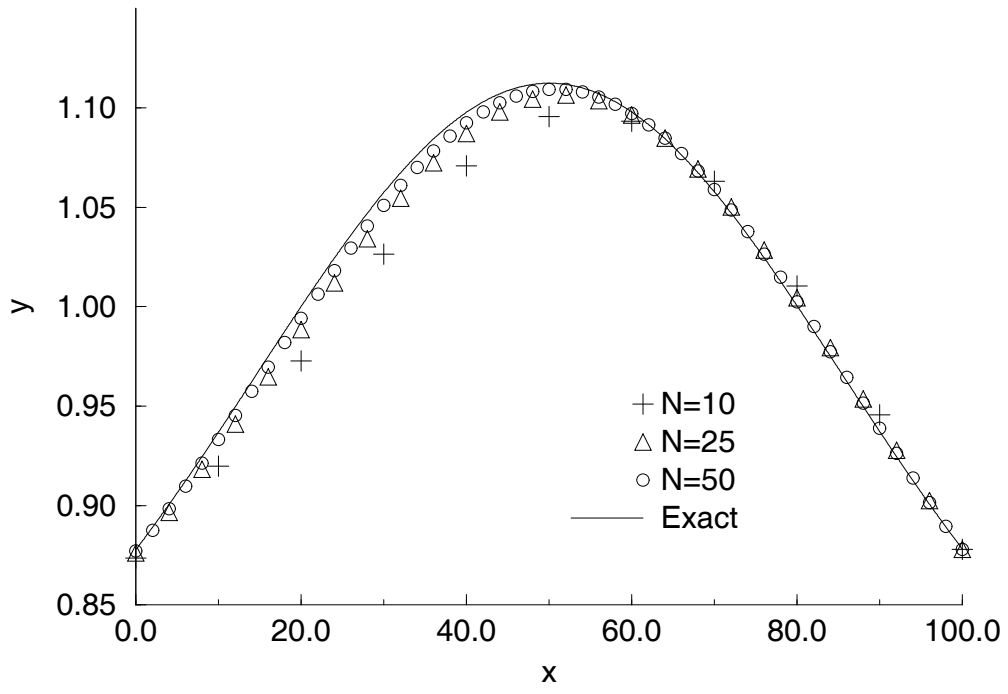


Figure 6: Numerical solutions against exact solution for problem 1

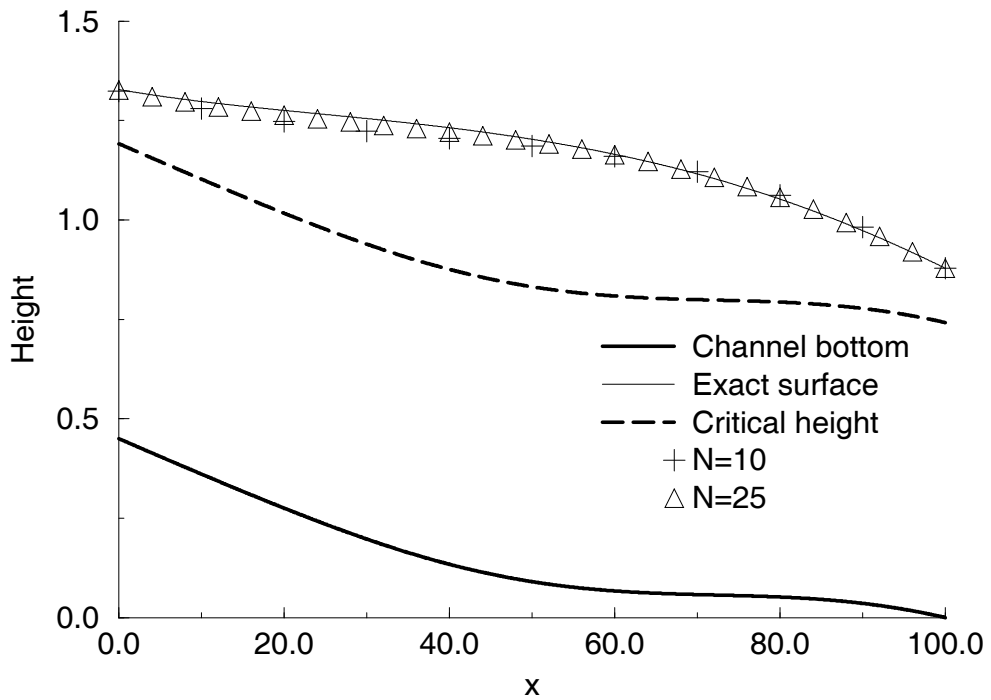


Figure 7: Computed free surfaces against exact free surface for problem 2

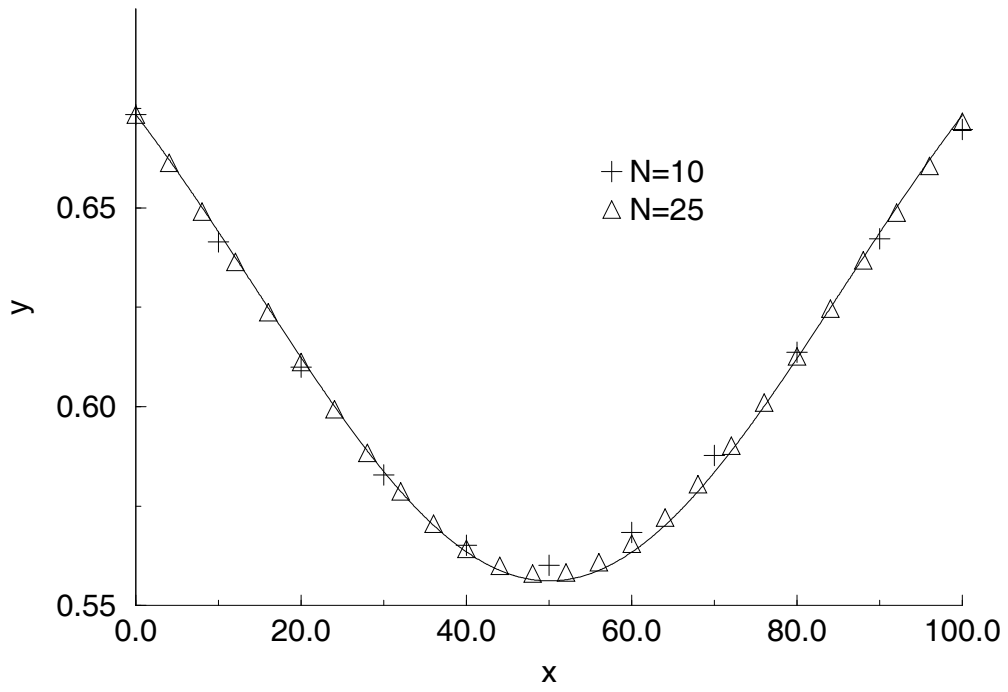


Figure 8: Numerical solutions against exact solution for problem 2

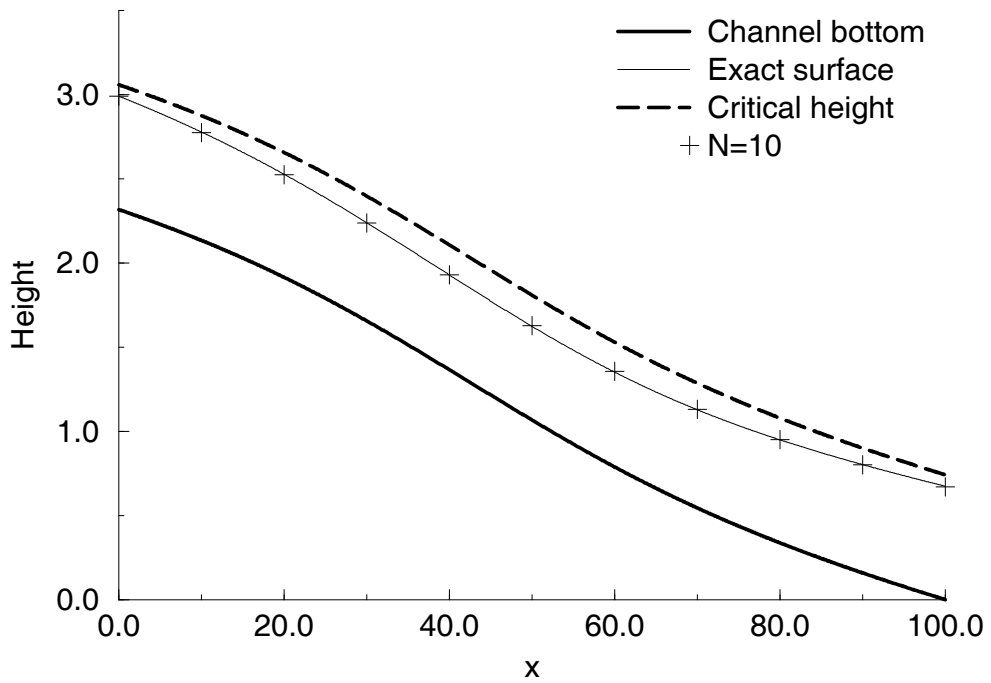


Figure 9: Computed free surface against exact free surface for problem 2

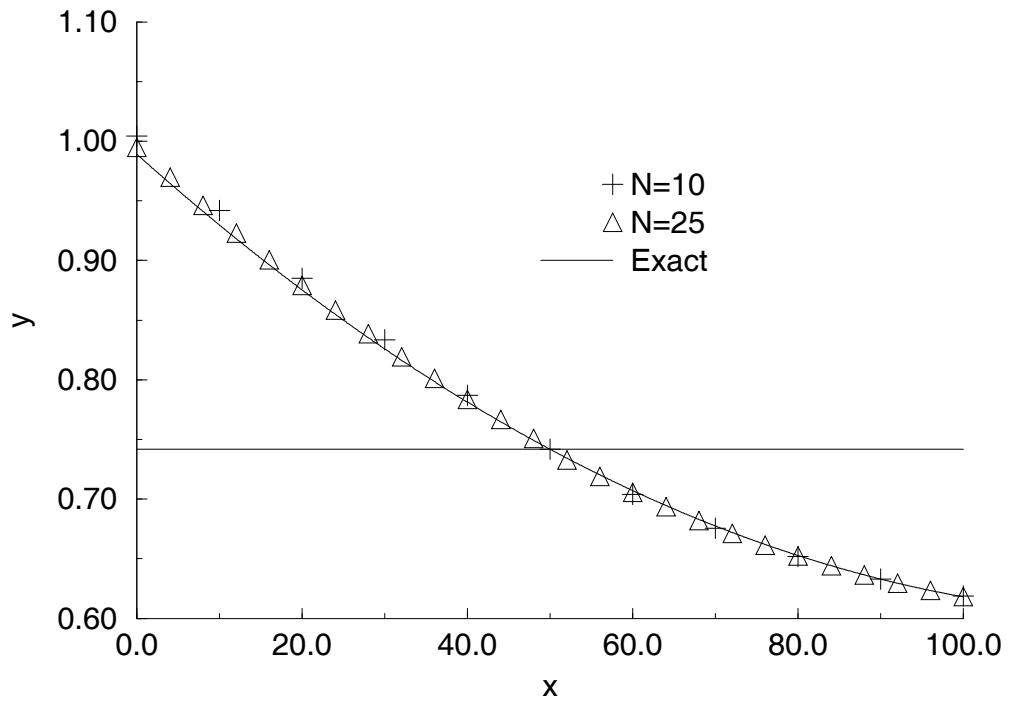


Figure 10: Numerical solutions against exact solution for problem 3

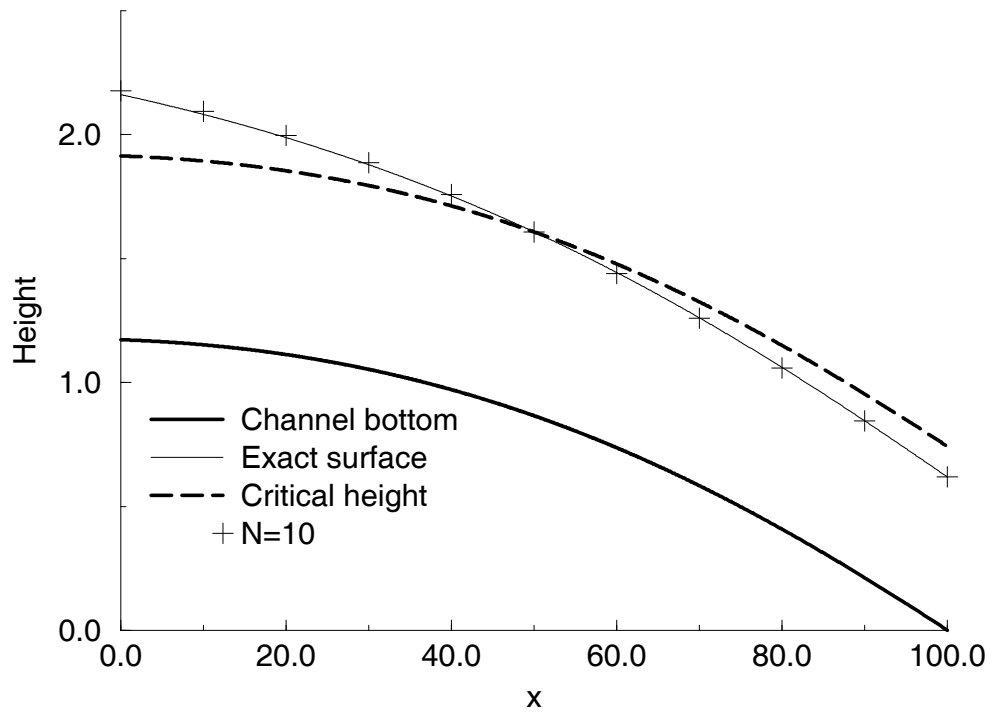


Figure 11: Computed free surface against exact free surface for problem 3

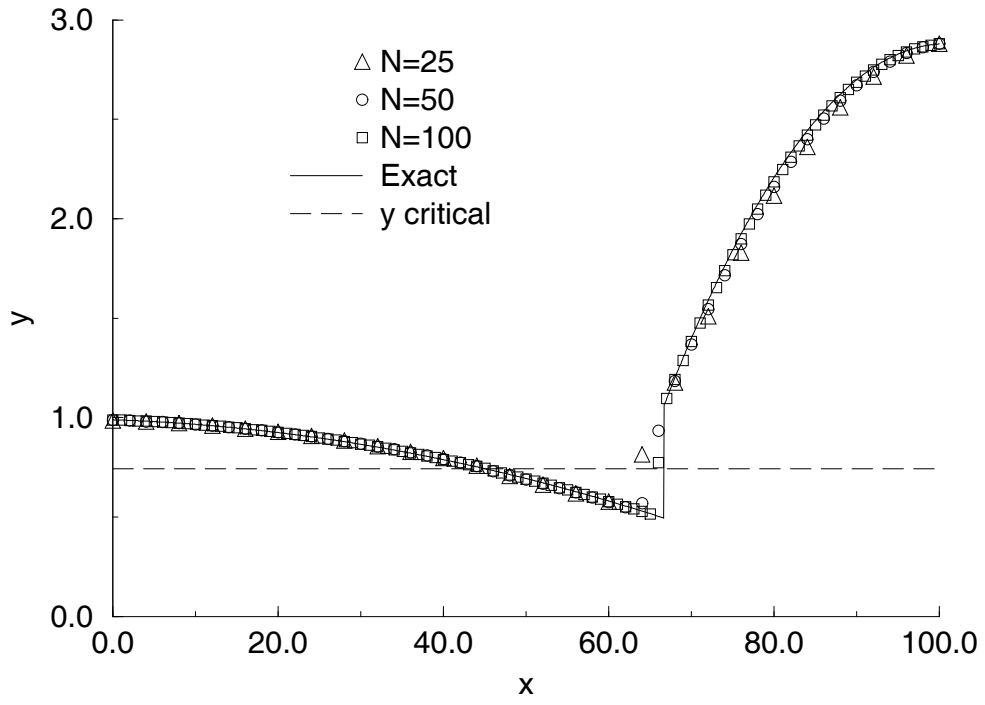


Figure 12: Numerical solutions against exact solution for problem 4

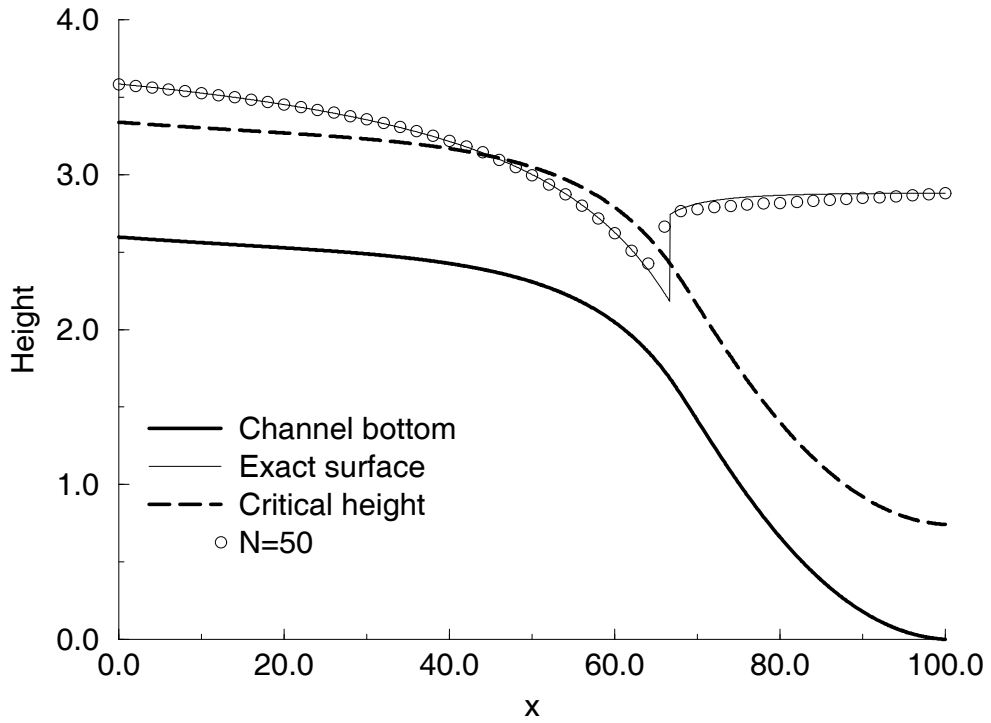


Figure 13: Computed free surface against exact free surface for problem 4

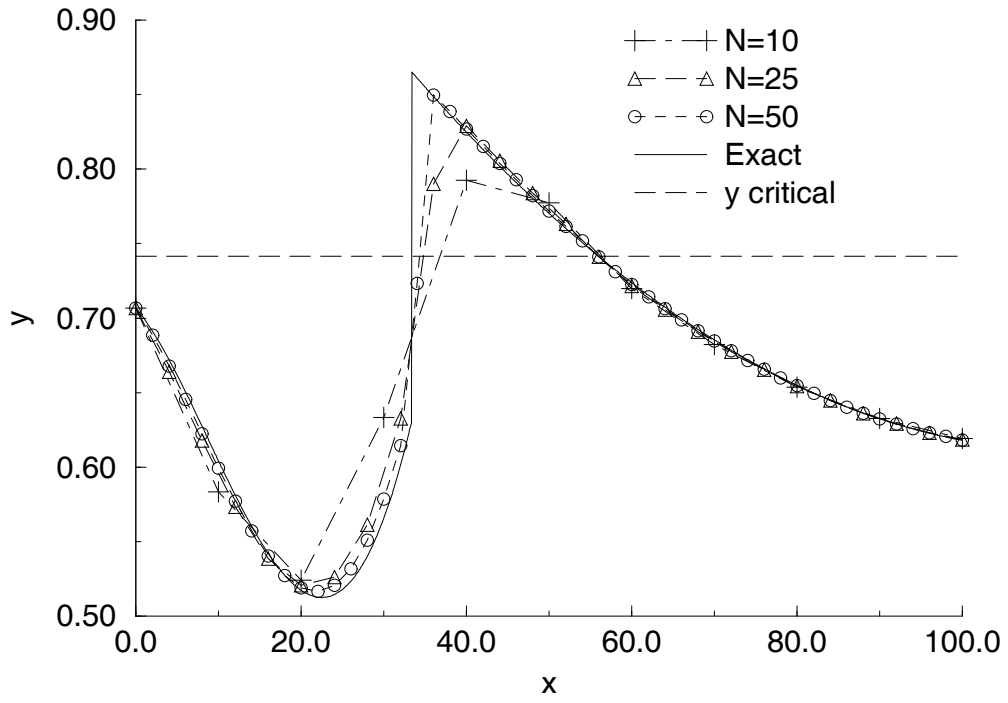


Figure 14: Numerical solutions against exact solution for problem 5

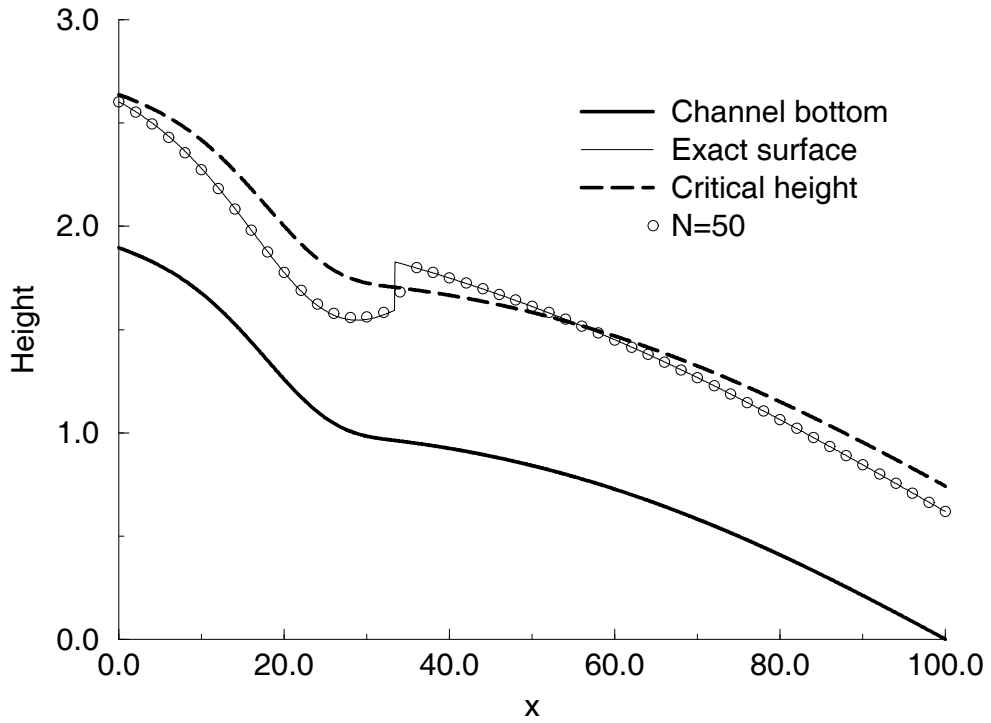


Figure 15: Computed free surface against exact free surface for problem 5

5 Analysis of a Class of Singular Perturbation Problems

In this section we prove a number of results concerning the problem

$$\epsilon \frac{d^2 y_\epsilon}{dx^2} - \frac{d}{dx} f(y_\epsilon) - b(x, y_\epsilon) = 0, \quad y_\epsilon(x) > 0, \quad 0 \leq x \leq 1, \quad (5.41)$$

$$y_\epsilon(0) = \gamma_0, \quad y_\epsilon(1) = \gamma_1,$$

where $\epsilon, \gamma_0, \gamma_1 > 0$, which are relevant to the steady Saint-Venant problem and have already been used in section 2. Here $b_x, b_y, b_{xy} \in C^0([0, 1] \times \mathbb{R}_+)$, $f \in C^2(\mathbb{R}_+)$ and we have

$$b_y(x, y) > 0, \quad \forall (x, y) \in [0, 1] \times \mathbb{R}_+. \quad (5.42)$$

We also assume that there exist $m, M > 0$ such that

$$\begin{aligned} (x, y) \in [0, 1] \times (0, m] &\implies b(x, y) \leq 0, \\ (x, y) \in [0, 1] \times [M, \infty) &\implies b(x, y) \geq 0. \end{aligned} \quad (5.43)$$

We let $\underline{y} = \min\{\gamma_0, \gamma_1, m\}$ and $\overline{y} = \max\{\gamma_0, \gamma_1, M\}$.

This problem without the solution restricted to being positive is well known, for example see Lorenz[8][9]. The existing results do not directly apply to our problem because they require the functions f and b to be defined for all y . We are particularly interested in problems where these functions are singular at $y = 0$. In order to use the existing analysis we construct another problem from (5.41) to which we can apply the existing results. Then, because of the way our new problem has been constructed, we can infer information about the original problem.

The intermediate problem we shall consider is as follows:

$$\epsilon \frac{d^2 \tilde{y}_\epsilon}{dx^2} - \frac{d}{dx} \tilde{f}(\tilde{y}_\epsilon) - \tilde{b}(x, \tilde{y}_\epsilon) = 0, \quad 0 \leq x \leq 1, \quad (5.44)$$

$$\tilde{y}_\epsilon(0) = \gamma_0, \quad \tilde{y}_\epsilon(1) = \gamma_1.$$

We define the functions \tilde{f} and \tilde{b} by

$$\tilde{f}(y) = \begin{cases} \left[\frac{1}{2}(f''(\overline{y}) + 2f'(\overline{y}) + f(\overline{y}))(y - \overline{y})^2 \right. \\ \left. + (f'(\overline{y}) + f(\overline{y}))(y - \overline{y}) + f(\overline{y}) \right] e^{-(y-\overline{y})} & y > \overline{y} \\ f(y) & \underline{y} \leq y \leq \overline{y} \\ \left[\frac{1}{2}(f''(\underline{y}) - 2f'(\underline{y}) + f(\underline{y}))(y - \underline{y})^2 \right. \\ \left. + (f'(\underline{y}) - f(\underline{y}))(y - \underline{y}) + f(\underline{y}) \right] e^{(y-\underline{y})} & y < \underline{y} \end{cases}, \quad (5.45)$$

and

$$\tilde{b}(x, y) = \begin{cases} b(x, \overline{y}) + (y - \overline{y})b_y(x, \overline{y}) & y > \overline{y} \\ b(x, y) & \underline{y} \leq y \leq \overline{y} \\ b(x, \underline{y}) + (y - \underline{y})b_y(x, \underline{y}) & y < \underline{y} \end{cases}. \quad (5.46)$$

It is not hard to see that $\tilde{f} \in C^2(\mathbb{R})$, $\tilde{b} \in C^1([0, 1] \times \mathbb{R})$ and also that

$$\tilde{b}_y(x, y) \geq \tilde{\delta} > 0, \quad \forall (x, y) \in [0, 1] \times \mathbb{R}, \quad (5.47)$$

where $\tilde{\delta} = \min\{b_y : (x, y) \in [0, 1] \times [\underline{y}, \overline{y}]\}$.

Theorem 1 Existence and Uniqueness

Problem (5.41) has a unique solution, $y_\epsilon \in C^2[0, 1]$, for all $\epsilon > 0$. This solution satisfies

$$\underline{y} \leq y_\epsilon(x) \leq \bar{y}, \quad 0 \leq x \leq 1. \quad (5.48)$$

Proof.

Lorenz[8] proves that problem (5.44) has a unique solution, $\tilde{y}_\epsilon \in C^2[0, 1]$. Clearly if we can show that this solution satisfies the bound

$$\underline{y} \leq \tilde{y}_\epsilon(x) \leq \bar{y}, \quad 0 \leq x \leq 1, \quad (5.49)$$

then it is also a solution of problem (5.41).

Suppose that $\max\{\tilde{y}_\epsilon(x) : 0 \leq x \leq 1\} > \bar{y}$, then \tilde{y}_ϵ must have a maximum turning point at $x^* \in (0, 1)$, say, where $\tilde{y}'_\epsilon(x^*) = 0$, $\tilde{y}''_\epsilon(x^*) \leq 0$. Now using the differential equation we have

$$\begin{aligned} \tilde{b}(x^*, \tilde{y}_\epsilon(x^*)) &= \epsilon \tilde{y}''_\epsilon(x^*) + \left. \frac{d}{dx} \tilde{f}(\tilde{y}_\epsilon(x)) \right|_{x=x^*} \\ &= \epsilon \tilde{y}''_\epsilon(x^*) + \tilde{f}'(\tilde{y}_\epsilon(x^*)) \tilde{y}'_\epsilon(x^*) \\ &= \epsilon \tilde{y}''_\epsilon(x^*) \\ &\leq 0. \end{aligned}$$

This is a contradiction since $y > M$ implies $\tilde{b}(x, y) > 0$. The same type of argument also gives the lower bound.

We have now shown that (5.41) has at least one solution, next we show that this solution is unique. Let y_ϵ be a solution to (5.41), then using the same argument as above we get the bound

$$\underline{y} \leq y_\epsilon(x) \leq \bar{y}, \quad 0 \leq x \leq 1,$$

and hence y_ϵ is also a solution to (5.44), implying that we must have $y_\epsilon \equiv \tilde{y}_\epsilon$. This completes the proof.

In this work we are mostly interested in solutions of the reduced equation ($\epsilon \rightarrow 0$), which under certain circumstances are relevant to the steady Saint-Venant problem. The remaining theory in this section concerns the limit $\epsilon \rightarrow 0$ of solutions to problem (5.41).

Now let the set NBV be given by

$$NBV = \{y \in BV : y(x) = y(x+) \forall x \in [0, 1) \text{ and } y(1) = y(1-)\}. \quad (5.50)$$

BV is the set of all functions of finite variation on $[0, 1]$. The set NBV is well defined, since for functions of finite variation, the limits from the left and right always exist for interior points, although only from the right at $x = 0$ and the left at $x = 1$; see Stromberg[16].

Lemma 1 *Let $Y \in NBV$ and let $\{\epsilon_n\}$ be a positive null sequence with $y_{\epsilon_n} \rightarrow Y$ a.e. as $n \rightarrow \infty$. Then Y has the bound*

$$\underline{y} \leq Y(x) \leq \bar{y}, \quad 0 \leq x \leq 1. \quad (5.51)$$

Proof.

Suppose $x \in [0, 1)$. Let $r_k = (1 - x)/k$ and consider the sequence of intervals given by $I_k = [x, x + r_k)$ for $k \in \mathbb{N}$. Since we have that $y_{\epsilon_n} \rightarrow Y$ a.e. as $n \rightarrow \infty$, we can find for each $k \in \mathbb{N}$, an $x_k \in I_k$ such that $y_{\epsilon_n}(x_k) \rightarrow Y(x_k)$ as $n \rightarrow \infty$. Now because of the bound (5.48) we have that $\underline{y} \leq Y(x_k) \leq \bar{y}$. Clearly $x_k \geq x$ and $x_k \rightarrow x$ as $k \rightarrow \infty$, so we have that $Y(x_k) \rightarrow Y(x)$ as $k \rightarrow \infty$, since $Y \in NBV$. This gives the bound. We can use the same principle to prove the bound for $x = 1$.

We now give four important theorems. These can be all proved by applying the corresponding theorems in Lorenz[8][9] to problem (5.44) and then using the fact that $y_\epsilon = \tilde{y}_\epsilon \forall \epsilon > 0$ and the bound given by lemma (1) to remove the tildes.

Theorem 2 *Let $\{\epsilon_n\}$ be a positive null sequence, then there is a subsequence $\{\epsilon_{n_k}\}$ and a function $Y \in NBV$ such that*

$$y_{\epsilon_{n_k}} \rightarrow Y \quad \text{a.e. as } k \rightarrow \infty. \quad (5.52)$$

Theorem 3 *Let $Y \in NBV$ and let $\{\epsilon_n\}$ be a positive null sequence with $y_{\epsilon_n} \rightarrow Y$ a.e. as $n \rightarrow \infty$. Y satisfies the following three conditions*

$$(i) \int_0^1 \{f(Y)\phi' - b(x, Y)\phi\} dx = 0 \quad \forall \phi \in C_0^\infty(0, 1).$$

$$(ii) \text{ For all discontinuities } x \in (0, 1) \text{ of } Y \text{ } sg(Y(x+) - Y(x-))(f(Y(x)) - f(k)) \leq 0 \text{ holds for all } k \text{ between } Y(x+) \text{ and } Y(x-).$$

$$(iii) \text{ At the boundary points } i = 0 \text{ and } i = 1 \text{ } 0 \leq (-1)^{i+1} sg(Y(i) - \gamma_i)(f(Y(i)) - f(k)) \text{ holds for all } k \text{ between } Y(i) \text{ and } \gamma_i.$$

Theorem 4 *There is a unique function $Y \in NBV$ that satisfies conditions (i), (ii) and (iii) in theorem 3.*

An equivalent characterisation of the limit function, Y , which is more useful for applications is given below. Roughly speaking it requires that Y satisfies the reduced differential equation

$$-\frac{d}{dx}f(Y(x)) - b(x, Y(x)) = 0, \quad (5.53)$$

in the smooth parts and Y obeys certain jump conditions at discontinuities and at the boundaries. The precise result follows.

Theorem 5 *A function $Y \in NBV$ satisfies conditions (i), (ii) and (iii) in theorem 3 if and only if the following holds:*

$$(i) \text{ If } I \text{ is an interval where } Y \text{ is continuous, then } f(Y(x)) \text{ is differentiable on } I, \text{ onesided in end points, and differential equation (5.53) holds on } I.$$

$$(ii) \text{ If } Y \text{ is discontinuous at } x \in (0, 1), \text{ then}$$

$$\begin{aligned} f(Y(x-)) &= f(Y(x+)) \geq f(k) & \text{if } Y(x-) > Y(x+), \\ f(Y(x-)) &= f(Y(x+)) \leq f(k) & \text{if } Y(x-) < Y(x+), \end{aligned} \quad (5.54)$$

for all k between $Y(x-)$ and $Y(x+)$.

$$(iii) \text{ For } i = 0, 1 \text{ and } k \text{ between } Y(i) \text{ and } \gamma_i$$

$$0 \leq (-1)^{i+1} sg(Y(i) - \gamma_i)(f(Y(i)) - f(k)). \quad (5.55)$$

6 Analysis of a Class of Monotone Difference Schemes for the Singular Perturbation Problem

In this section we analyse a family of numerical schemes for solving problem (5.41). We consider a uniform grid $x_i = i/h$, $i = 0, 1, \dots, N$ and the difference scheme

$$\frac{\epsilon}{h^2}(u_{i+1} - 2u_i + u_{i-1}) - \frac{1}{h}(g(u_{i+1}, u_i) - g(u_i, u_{i-1})) - b(x_i, u_i) = 0, \quad (6.56)$$

$$i = 1, \dots, N - 1,$$

$$u_0 = \gamma_0, \quad u_N = \gamma_1.$$

Here the ‘‘numerical flux function’’ $g(u, v) \in C^0(\mathbb{R}_+^2)$ is subject to consistency and monotonicity conditions

$$g(u, u) = f(u), \quad (6.57)$$

$$\begin{aligned} u &\rightarrow g(u, v) \text{ is nonincreasing,} \\ v &\rightarrow g(u, v) \text{ is nondecreasing.} \end{aligned} \quad (6.58)$$

We also require that, for any bounded set $\Omega \subset \mathbb{R}_+^2$, there is a constant $L_\Omega > 0$ such that for all $[u_1, v_1]^T, [u_2, v_2]^T \in \Omega$,

$$|g(u_1, v_1) - g(u_2, v_2)| \leq L_\Omega(|u_1 - u_2| + |v_1 - v_2|). \quad (6.59)$$

We shall be most interested in the C^1 numerical flux function of Engquist-Osher given by

$$g(u, v) = \int_c^u \min\{f'(s), 0\} ds + \int_c^v \max\{f'(s), 0\} ds, \quad (6.60)$$

where $c > 0$ is some arbitrary value.

6.1 Existence and Uniqueness of Discrete Solution

Lemma 2 *Let $\Omega = [y_L, y_R]^2 \subset \mathbb{R}_+^2$. Then for any $u_1, v_1, u_2, v_2 \in [y_L, y_R]$*

$$g(u_1, v_1) - g(u_2, v_2) = (u_1 - u_2)L^u(u_1, u_2, v_1) + (v_1 - v_2)L^v(v_1, v_2, u_2),$$

where

$$\begin{aligned} L^u(s_1, s_2, s_3) &= \begin{cases} 0 & \text{if } s_1 = s_2 \\ \frac{g(s_1, s_3) - g(s_2, s_3)}{s_1 - s_2} & \text{if } s_1 \neq s_2, \end{cases} \\ L^v(s_1, s_2, s_3) &= \begin{cases} 0 & \text{if } s_1 = s_2 \\ \frac{g(s_3, s_1) - g(s_3, s_2)}{s_1 - s_2} & \text{if } s_1 \neq s_2, \end{cases} \end{aligned}$$

and

$$\begin{aligned} 0 &\leq -L^u(u_1, u_2, v_1) \leq L_\Omega, \\ 0 &\leq L^v(v_1, v_2, u_2) \leq L_\Omega. \end{aligned}$$

The proof is trivial and will be omitted.

Lemma 3 Let $0 < y_L \leq y_R$, $h > 0$ and $\epsilon \geq 0$. There exists a value $\Delta t_{y_L, y_R}^{\epsilon, h} > 0$ such that, for $0 < \Delta t < \Delta t_{y_L, y_R}^{\epsilon, h}$,

$$\Delta t \left[\frac{2\epsilon}{h^2} + \frac{1}{h} (L^v(s_1, s_2, s_3) - L^u(s_1, s_2, s_4)) + b_y(x, s_5) \right] < 1, \quad (6.61)$$

for all $s_1, s_2, s_3, s_4, s_5 \in [y_L, y_R]$, $x \in [0, 1]$.

Proof.

Let

$$\bar{b}_y = \max\{b_y(x, y) : (x, y) \in [0, 1] \times [y_L, y_R]\} > 0. \quad (6.62)$$

Now let

$$\Delta t_{y_L, y_R}^{\epsilon, h} = \left[\frac{2\epsilon}{h^2} + \frac{2}{h} L_\Omega + \bar{b}_y \right]^{-1},$$

where $\Omega = [y_L, y_R]^2$. It is easily seen that this value satisfies the lemma.

Lemma 4 Let $0 < y_L \leq \underline{y}$, $y_R \geq \bar{y}$, $\epsilon \geq 0$ and $h = 1/N$, where $N - 1 \in \mathbb{N}$. Let us define the set

$$\Lambda_{y_L, y_R}^{N+1} = \left\{ \mathbf{u} = [u_0, u_1, \dots, u_N]^T \in \mathbb{R}^{N+1} : u_0 = \gamma_0, u_N = \gamma_1, y_L \leq \mathbf{u} \leq y_R \right\} \quad (6.63)$$

and the operator $\mathbf{G} : \mathbb{R}_+^{N+1} \rightarrow \mathbb{R}^{N+1}$ by

$$\mathbf{G}(\mathbf{u})|_i = \begin{cases} \gamma_0 & i = 0, \\ u_i + \Delta t (T_h^\epsilon \mathbf{u})_i & i = 1, \dots, N-1, \\ \gamma_1 & i = N, \end{cases} \quad (6.64)$$

where

$$(T_h^\epsilon \mathbf{u})_i = \frac{\epsilon}{h^2} (u_{i+1} - 2u_i + u_{i-1}) - \frac{1}{h} (g(u_{i+1}, u_i) - g(u_i, u_{i-1})) - b(x_i, u_i) \quad (6.65)$$

and $0 < \Delta t < \Delta t_{y_L, y_R}^{\epsilon, h}$. Then we have the following:

- (i) $\mathbf{u}, \mathbf{v} \in \mathbb{R}^{N+1}$, $y_L \leq \mathbf{u} \leq \mathbf{v} \leq y_R \implies \mathbf{G}(\mathbf{u}) \leq \mathbf{G}(\mathbf{v})$.
- (ii) $\mathbf{G}(\Lambda_{y_L, y_R}^{N+1}) \subset \Lambda_{y_L, y_R}^{N+1}$.
- (iii) $\mathbf{u}, \mathbf{v} \in \Lambda_{y_L, y_R}^{N+1} \implies \|\mathbf{G}(\mathbf{u}) - \mathbf{G}(\mathbf{v})\|_1 \leq (1 - \Delta t \delta_{y_L, y_R}) \|\mathbf{u} - \mathbf{v}\|_1$,

where

$$\delta_{y_L, y_R} = \min\{b_y(x, y) : (x, y) \in [0, 1] \times [y_L, y_R]\}. \quad (6.66)$$

Note that $0 < 1 - \Delta t \delta_{y_L, y_R} < 1$.

Proof.

(i). Let $\mathbf{u}, \mathbf{v} \in \mathbb{R}^{N+1}$, with $y_L \leq \mathbf{u} \leq \mathbf{v} \leq y_R$. Now for $1 \leq i \leq N-1$

$$\begin{aligned} \mathbf{G}(\mathbf{v})|_i - \mathbf{G}(\mathbf{u})|_i &= w_i + \frac{\epsilon \Delta t}{h^2} (w_{i+1} - 2w_i + w_{i-1}) \\ &\quad - \frac{\Delta t}{h} (g(v_{i+1}, v_i) - g(u_{i+1}, u_i)) + \frac{\Delta t}{h} (g(v_i, v_{i-1}) - g(u_i, u_{i-1})) \end{aligned}$$

$$-\Delta t(b(x, v_i) - b(x, u_i)),$$

where $w_i = v_i - u_i$. Using lemma 2 and the mean value theorem, this can be written as

$$\begin{aligned} \mathbf{G}(\mathbf{v})|_i - \mathbf{G}(\mathbf{u})|_i &= w_{i-1} \Delta t \left[\frac{\epsilon}{h^2} + \frac{1}{h} L^v(v_{i-1}, u_{i-1}, u_i) \right] \\ &+ w_i \left[1 - \Delta t \left(\frac{2\epsilon}{h^2} - \frac{1}{h} L^u(v_i, u_i, v_{i-1}) + \frac{1}{h} L^v(v_i, u_i, u_{i+1}) + b_y(x_i, \bar{w}_i) \right) \right] \\ &+ w_{i+1} \Delta t \left[\frac{\epsilon}{h^2} - \frac{1}{h} L^u(v_{i+1}, u_{i+1}, v_i) \right], \end{aligned} \quad (6.67)$$

where $y_L \leq \bar{w}_i \leq y_R$. Since all the w_i are non-negative, the first and last term are easily seen to be non-negative. Also by lemma 3 the second term is also non-negative. Hence we have the required result

$$\mathbf{G}(\mathbf{u}) \leq \mathbf{G}(\mathbf{v}),$$

since $\mathbf{G}(\mathbf{v})|_0 = \mathbf{G}(\mathbf{u})|_0 = \gamma_0$ and $\mathbf{G}(\mathbf{v})|_N = \mathbf{G}(\mathbf{u})|_N = \gamma_1$.

(ii). Let $\mathbf{y}_L = [y_L, y_L, \dots, y_L]^T \in \mathbb{R}^{N+1}$, then for $1 \leq i \leq N-1$

$$\mathbf{G}(\mathbf{y}_L)|_i = y_L - \Delta t b(x_i, y_L) \geq y_L,$$

by (5.43), $\mathbf{G}(\mathbf{y}_L)|_0 = \gamma_0 \geq y_L$ and $\mathbf{G}(\mathbf{y}_L)|_N = \gamma_1 \geq y_L$. Similarly, for $\mathbf{y}_R = [y_R, y_R, \dots, y_R]^T \in \mathbb{R}^{N+1}$, for $1 \leq i \leq N-1$

$$\mathbf{G}(\mathbf{y}_R)|_i = y_R - \Delta t b(x_i, y_R) \leq y_R,$$

by (5.43), $\mathbf{G}(\mathbf{y}_R)|_0 = \gamma_0 \leq y_R$ and $\mathbf{G}(\mathbf{y}_R)|_N = \gamma_1 \leq y_R$. Now let $\mathbf{u} \in \Lambda_{y_L, y_R}^{N+1}$, then

$$y_L \leq \mathbf{y}_L \leq \mathbf{u} \leq \mathbf{y}_R \leq y_R,$$

and so by (i) we have

$$y_L \leq \mathbf{G}(\mathbf{y}_L) \leq \mathbf{G}(\mathbf{u}) \leq \mathbf{G}(\mathbf{y}_R) \leq y_R.$$

(iii). Let $\mathbf{u}, \mathbf{v} \in \Lambda_{y_L, y_R}^{N+1}$. Taking absolute values of equation (6.67) and using the triangle inequality on the right hand side we obtain

$$\begin{aligned} |\mathbf{G}(\mathbf{v})|_i - \mathbf{G}(\mathbf{u})|_i| &\leq |w_{i-1}| \Delta t \left[\frac{\epsilon}{h^2} + \frac{1}{h} L^v(v_{i-1}, u_{i-1}, u_i) \right] \\ &+ |w_i| \left[1 - \Delta t \left(\frac{2\epsilon}{h^2} - \frac{1}{h} L^u(v_i, u_i, v_{i-1}) + \frac{1}{h} L^v(v_i, u_i, u_{i+1}) + b_y(x_i, \bar{w}_i) \right) \right] \\ &+ |w_{i+1}| \Delta t \left[\frac{\epsilon}{h^2} - \frac{1}{h} L^u(v_{i+1}, u_{i+1}, v_i) \right], \end{aligned} \quad (6.68)$$

$i = 1, \dots, N-1$. Summing this equation from $i = 1$ to $i = N-1$, we find that the sum telescopes, giving

$$\sum_{i=1}^{i=N-1} |\mathbf{G}(\mathbf{v})|_i - \mathbf{G}(\mathbf{u})|_i| \leq \sum_{i=1}^{i=N-1} |w_i| (1 - \Delta t b_y(x_i, \bar{w}_i))$$

$$\begin{aligned}
& +|w_0|\Delta t \left[\frac{\epsilon}{h^2} + \frac{1}{h}L^v(v_0, u_0, u_1) \right] + |w_N|\Delta t \left[\frac{\epsilon}{h^2} - \frac{1}{h}L^u(v_N, u_N, v_{N-1}) \right] \\
& -|w_1|\Delta t \left[\frac{\epsilon}{h^2} - \frac{1}{h}L^u(v_1, u_1, v_0) \right] - |w_{N-1}|\Delta t \left[\frac{\epsilon}{h^2} + \frac{1}{h}L^v(v_{N-1}, u_{N-1}, u_N) \right].
\end{aligned}$$

Now, using the fact that $w_0 = w_N = |\mathbf{G}(\mathbf{v})|_0 - \mathbf{G}(\mathbf{u})|_0 = |\mathbf{G}(\mathbf{v})|_N - \mathbf{G}(\mathbf{u})|_N = 0$ and leaving out the two negative terms, we arrive at

$$\sum_{i=0}^{i=N} |\mathbf{G}(\mathbf{v})|_i - \mathbf{G}(\mathbf{u})|_i \leq \sum_{i=0}^{i=N} |w_i| (1 - \Delta t b_y(x, \bar{w}_i)) \leq (1 - \Delta t \delta_{y_L, y_R}) \sum_{i=0}^{i=N} |w_i|.$$

This completes the proof.

Theorem 6 *Let $\epsilon \geq 0$, $h = 1/N$, where $N - 1 \in \mathbb{N}$. Then there is a unique $\mathbf{u}_h^\epsilon = [u_0^{\epsilon, h}, u_1^{\epsilon, h}, \dots, u_N^{\epsilon, h}]^T \in \mathbb{R}_+^{N+1}$ satisfying system (6.56), and*

$$\underline{y} \leq \mathbf{u}_h^\epsilon \leq \bar{y}. \tag{6.69}$$

Proof

Let $y_L = \underline{y}$ and $y_R = \bar{y}$. By lemma 4, $\mathbf{G} : \Lambda_{\underline{y}, \bar{y}}^{N+1} \longrightarrow \Lambda_{\underline{y}, \bar{y}}^{N+1}$ is a contraction mapping in the L_1 norm and, by the contraction mapping theorem, \mathbf{G} has a unique fixed point in $\Lambda_{\underline{y}, \bar{y}}^{N+1}$. By definition this fixed point must be a solution to the system of equations (6.56).

Now suppose that the system of equations (6.56) has more than one solution in \mathbb{R}_+^{N+1} . Then there exist $0 < y_L \leq \underline{y}$ and $y_R \geq \bar{y}$ such that Λ_{y_L, y_R}^{N+1} contains multiple solutions. As above we can apply lemma 4 to show that $\mathbf{G} : \Lambda_{y_L, y_R}^{N+1} \longrightarrow \Lambda_{y_L, y_R}^{N+1}$ has a unique fixed point in this set. This is a contradiction, and completes the proof.

Theorem 7 *Let $\epsilon \geq 0$, $h = 1/N$, where $N - 1 \in \mathbb{N}$, $\mathbf{u}^0 = [u_0^0, u_1^0, \dots, u_N^0]^T \in \mathbb{R}_+^{N+1}$, with $u_0^0 = \gamma_0, u_N^0 = \gamma_1$. If $y_L = \min\{\underline{y}, u_1^0, u_2^0, \dots, u_{N-1}^0\}$ and $y_R = \max\{\bar{y}, u_1^0, u_2^0, \dots, u_{N-1}^0\}$, then the sequence of vectors $\{\mathbf{u}^n\}_{n=0}^\infty$ given by*

$$\mathbf{u}^{n+1} = \mathbf{G}(\mathbf{u}^n), \quad n > 0,$$

where $\mathbf{G} : \Lambda_{y_L, y_R}^{N+1} \longrightarrow \Lambda_{y_L, y_R}^{N+1}$ is given by lemma 4, converges in L_1 to the solution, \mathbf{u}_h^ϵ , of system (6.56) and we have that

$$\|\mathbf{u}^n - \mathbf{u}_h^\epsilon\|_1 \leq \exp(-n\Delta t \delta_{y_L, y_R}) \|\mathbf{u}^0 - \mathbf{u}_h^\epsilon\|_1, \tag{6.70}$$

where δ_{y_L, y_R} is given by (6.66).

Proof.

From lemma 4 we have

$$\|\mathbf{u}^{n+1} - \mathbf{u}_h^\epsilon\|_1 = \|\mathbf{G}(\mathbf{u}^n) - \mathbf{G}(\mathbf{u}_h^\epsilon)\|_1 \leq (1 - \Delta t \delta_{y_L, y_R}) \|\mathbf{u}^n - \mathbf{u}_h^\epsilon\|_1,$$

hence

$$\|\mathbf{u}^n - \mathbf{u}_h^\epsilon\|_1 \leq (1 - \Delta t \delta_{y_L, y_R})^n \|\mathbf{u}^0 - \mathbf{u}_h^\epsilon\|_1 \leq \exp(-n\Delta t \delta_{y_L, y_R}) \|\mathbf{u}^0 - \mathbf{u}_h^\epsilon\|_1.$$

The convergence is trivial, since $\Delta t \delta_{y_L, y_R} > 0$

6.2 Convergence as $h, \epsilon \rightarrow 0$

In section 5 we proved the existence of a unique physical solution, $Y \in NBV$, of the reduced problem ($\epsilon \rightarrow 0$). We now give a theorem that shows that, if we apply the above numerical scheme then, as $\epsilon \rightarrow 0$, the numerical solution is guaranteed to converge to Y .

Theorem 8 *Let $\mathbf{u}_h^0 = [u_0^{0,h}, u_1^{0,h}, \dots, u_N^{0,h}]^T$ denote the discrete solution of (6.56) for $\epsilon = 0$ and let U^h be the piecewise constant function*

$$U^h(x) = u_i^{0,h} \text{ for } ih \leq x \leq ih + h, \quad i = 0, 1, \dots, N-1. \quad (6.71)$$

Let $\{h_n\}$ be a null sequence where each $h_n = 1/(j+1)$ for some $j \in \mathbb{N}$, then there is a subsequence $\{h_{n_k}\}$ such that

$$U^{h_{n_k}} \rightarrow Y \in NBV \quad \text{a.e. as } k \rightarrow \infty. \quad (6.72)$$

Y is the unique function in NBV that satisfies conditions (i),(ii) and (iii) in theorem 3.

Proof.

To prove this result we take the same approach as in the analysis in section 5. We look at the numerical scheme

$$\frac{\epsilon}{h^2} (u_{i+1} - 2u_i + u_{i-1}) - \frac{1}{h} (\tilde{g}(u_{i+1}, u_i) - \tilde{g}(u_i, u_{i-1})) - \tilde{b}(x_i, u_i) = 0, \quad (6.73)$$

$$i = 1, \dots, N-1,$$

$$u_0 = \gamma_0, \quad u_N = \gamma_1,$$

for solving problem (5.44). Here \tilde{g} is given by

$$\tilde{g}(u, v) = \begin{cases} g(u, v) & \underline{y} \leq u \leq \bar{y} \text{ and } \underline{y} \leq v \leq \bar{y}, \\ g(\bar{y}, \bar{y}) + H_1(u; \bar{y}) + H_2(v; \bar{y}) & u > \bar{y} \text{ and } v > \bar{y}, \\ g(\bar{y}, v) + H_1(u; \bar{y}) & u > \bar{y} \text{ and } \underline{y} \leq v \leq \bar{y}, \\ g(\bar{y}, \underline{y}) + H_1(u; \bar{y}) + H_2(v; \underline{y}) & u > \bar{y} \text{ and } v < \underline{y}, \\ g(u, \underline{y}) + H_2(v; \underline{y}) & \underline{y} \leq u \leq \bar{y} \text{ and } v < \underline{y}, \\ g(\underline{y}, \underline{y}) + H_1(u; \underline{y}) + H_2(v; \underline{y}) & u < \underline{y} \text{ and } v < \underline{y}, \\ g(\underline{y}, v) + H_1(u; \underline{y}) & u < \underline{y} \text{ and } \underline{y} \leq v \leq \bar{y}, \\ g(\underline{y}, \bar{y}) + H_1(u; \underline{y}) + H_2(v; \bar{y}) & u < \underline{y} \text{ and } v > \bar{y}, \\ g(u, \bar{y}) + H_2(v; \bar{y}) & \underline{y} \leq u \leq \bar{y} \text{ and } v > \bar{y}, \end{cases} \quad (6.74)$$

where

$$H_1(u; z) = \int_z^u \min\{\tilde{f}'(s)\} ds, \quad (6.75)$$

and

$$H_2(v; z) = \int_z^v \max\{\tilde{f}'(s)\} ds. \quad (6.76)$$

Since $H_1(z; z) = 0$ and $H_2(z; z) = 0$ it can be shown that $\tilde{g} \in C^0(\mathbb{R}^2)$. It is not hard to see that $\tilde{g}(u, u) = f(u)$ for all $u \in \mathbb{R}$. Also $u \rightarrow H_1(u; z)$ is nonincreasing and $v \rightarrow H_2(v; z)$ is nondecreasing, so with our assumptions (6.58) about g , we have that $u \rightarrow \tilde{g}(u, v)$ is nonincreasing and that $v \rightarrow \tilde{g}(u, v)$ is nondecreasing. Moreover, $|\tilde{f}'(y)| \leq C$ for some constant C , so because of assumptions (6.59) and

the fact that H_1, H_2 have bounded derivatives, \tilde{g} satisfies a Lipschitz condition globally.

Now under these conditions, the system of equations (6.73) has a unique solution, $\tilde{\mathbf{u}}_h^\epsilon = [\tilde{u}_0^{\epsilon,h}, \tilde{u}_1^{\epsilon,h}, \dots, \tilde{u}_N^{\epsilon,h}]^T$, for $\epsilon \geq 0$ and $h = 1/N$, where $N - 1 \in \mathcal{N}$ (See Lorenz[8]). Because of the way \tilde{g} , \tilde{f} and \tilde{b} have been constructed and the bound on the solution of (6.56), we must have that $\tilde{\mathbf{u}}_h^\epsilon = \mathbf{u}_h^\epsilon$ where \mathbf{u}_h^ϵ is the solution of (6.56). Lorenz[8] proves the corresponding theorem for (6.73). The result follows because $\mathbf{u}_h^\epsilon = \tilde{\mathbf{u}}_h^\epsilon$.

7 Conclusions and Further Work

For a rectangular channel with positive bed slope, we have shown that the unique physical steady flow can be obtained as the zero viscosity limit of solutions to a sequence of viscous problems which are generated by adding an artificial viscosity term, of strength ϵ , to the steady Saint-Venant equations. By this limiting process we also obtained a family of numerical schemes which are guaranteed to converge to the physical solution in the limit as the grid size tends to zero. We demonstrated that these schemes are well behaved in the sense that the numerical solution always exists and is uniformly bounded. We have also given numerical results for a particular member of this class of schemes for a series of test problems. The results show that the numerical scheme approximates the solution well in smooth regions and also gives very good resolution of the discontinuities.

In the future we would like to extend the theory given in this report to a less restrictive class of channels. The extension of the analysis to certain other shapes of cross-section seems to be relatively simple. However, the extension to non-prismatic channels with non-positive bed slopes appears to be much more difficult. If it is possible, then it will require a different approach to the analysis given here. Nevertheless, even if we cannot extend the theory a great deal by the techniques given in this report, we are confident that we can generalise the numerical schemes given in this work to they apply to arbitrary channels, and in particular natural channels given by discrete data. After this we plan to modify the numerical schemes to work on non-uniform grids and eventually use some kind of adaption. In this way we hope to obtain a better resolution of the discontinuities without increasing the number of grid points.

Acknowledgements

Thanks to the SERC and HR Wallingford Ltd for funding this work.

References

- [1] U M Ascher, R M M Mattheij, and R D Russell. *Numerical Solution of Boundary Value Problems for Ordinary Differential Equations*. Prentice Hall, 1988.
- [2] Ven Te Chow. *Open Channel Hydraulics*. McGraw-Hill, 1959.
- [3] J A Cunge, F M Holly, and A Verwey. *Practical Aspects of Computational River Hydraulics*. Pitman, London, England, 1980.
- [4] Bjorn Engquist and Stanley Osher. Stable and entropy satisfying approximations for transonic flow calculations. *Mathematics of Computation*, 34(149):45–75, January 1980.
- [5] Bjorn Engquist and Stanley Osher. One-sided difference approximations for nonlinear conservation laws. *Mathematics of Computation*, 36(154):321–351, April 1981.
- [6] P Glaister. A comparison of three methods for solving singular perturbation problems. M.Sc. thesis, Department of Mathematics, University of Reading, 1982.
- [7] Randall J LeVeque. *Numerical Methods for Conservation Laws*. Birkhäuser Verlag, Basel, Boston, Berlin, 1990.
- [8] Jens Lorenz. Nonlinear boundary value problems with turning points and properties of difference schemes. *Lecture Notes in Applied Mathematics*, 942:150–169, 1982.
- [9] Jens Lorenz. Analysis of difference schemes for a stationary shock problem. *SIAM J. Numer. Anal.*, 21(6):1038–1053, December 1984.
- [10] Ian MacDonald. Test problems with analytic solutions for steady open channel flow. Numerical Analysis Report 6/94, Department of Mathematics, University of Reading, 1994.
- [11] Koichi Nijima. On a difference scheme of exponential type for a nonlinear perturbation problem. *Numer. Math.*, 46:521–539, 1985.
- [12] R E O'Malley. *Introduction to Singular Perturbations*. Academic Press, New York and London, 1974.
- [13] Stanley Osher. Nonlinear singular perturbation problems and one sided difference schemes. *SIAM J. Numer. Anal.*, 18(1):129–144, February 1981.
- [14] Stanley Osher. Numerical solution of singular perurbation problems and hyperbolic systems of conservation laws. In *Analytical and Numerical Approaches to Asymptotic Problems in Analysis*. North Holland Publishing Company, 1981.
- [15] Carl E Pearson. On the differential equation of boundary layer type. *J. Maths. Phys.*, 47:134–154, 1968.

- [16] Karl R Stromberg. *An Introduction to Classical Real Analysis*. Wadsworth International, Belmont, California, 1981.

A Notation

\mathbb{R}_+	$(0, \infty)$
\mathbf{u}	Bold denotes a vector
$\mathbf{u} _i$	i 'th component of vector
$\mathbf{u} \leq \alpha$	$\mathbf{u} _i \leq \alpha$ for all i ; same for $=, \geq, <$ and $>$
$\mathbf{u} \leq \mathbf{v}$	$\mathbf{u} _i \leq \mathbf{v} _i$ for all i ; same for $=, \geq, <$ and $>$
$\text{sg}(z)$	$\text{sg}(z) = -1, 0, 1$ for $z < 0, = 0, > 0$
$C^n(A)$	Set of functions $f : A \rightarrow \mathbb{R}$ that have n continuous derivatives
$u(x+)$	Limit $u(x + \delta)$, as $\delta \rightarrow 0$ from above
$u(x-)$	Limit $u(x - \delta)$, as $\delta \rightarrow 0$ from above
BV	Functions of Bounded Variation on $[0, 1]$
NBV	$\{u \in BV : u(x) = u(x+), \text{ for } x \in [0, 1), u(1) = u(1-)\}$
$C_0^\infty(0, 1)$	Smooth test functions with compact support on $(0, 1)$
$\ \mathbf{u}^h\ _1$	$h \sum_{i=0}^N u_i $

B Details of Test Problems

In this Appendix we give details of the test problems used in section 4. The exact solutions are illustrated in figures 6-15.

Problem 1 *Subcritical Flow*

A rectangular channel, $0 \leq x \leq 100m$, has width $10m$ and a discharge of $20m^3s^{-1}$. The slope of the channel is given by

$$S_0(x) = \left(1 - \frac{4}{g[\hat{y}(x)]^3}\right) \hat{y}'(x) + \frac{9}{2500[\hat{y}(x)]^2} \left(\frac{1}{5} + \frac{1}{\hat{y}(x)}\right)^{4/3},$$

where

$$\hat{y}(x) = \left(\frac{4}{g}\right)^{1/3} \left(1 + \frac{1}{2} \exp\left[-4\left(\frac{x}{100} - \frac{1}{2}\right)^2\right]\right),$$

and

$$\hat{y}'(x) = -\left(\frac{4}{g}\right)^{1/3} \frac{1}{25} \left(\frac{x}{100} - \frac{1}{2}\right) \exp\left[-4\left(\frac{x}{100} - \frac{1}{2}\right)^2\right].$$

Manning's friction coefficient for the channel is 0.03. The flow is subcritical at outflow, with depth $\hat{y}(100)$, and subcritical at inflow.

The exact solution for this problem is $y(x) \equiv \hat{y}(x)$.

Problem 2 *Supercritical Flow*

A rectangular channel, $0 \leq x \leq 100m$, has width $10m$ and a discharge of $20m^3s^{-1}$. The slope of the channel is given by

$$S_0(x) = \left(1 - \frac{4}{g[\hat{y}(x)]^3}\right) \hat{y}'(x) + \frac{9}{2500[\hat{y}(x)]^2} \left(\frac{1}{5} + \frac{1}{\hat{y}(x)}\right)^{4/3},$$

where

$$\hat{y}(x) = \left(\frac{4}{g}\right)^{1/3} \left(1 - \frac{1}{4} \exp\left[-4\left(\frac{x}{100} - \frac{1}{2}\right)^2\right]\right),$$

and

$$\hat{y}'(x) = \left(\frac{4}{g}\right)^{1/3} \frac{1}{50} \left(\frac{x}{100} - \frac{1}{2}\right) \exp\left[-4\left(\frac{x}{100} - \frac{1}{2}\right)^2\right].$$

Manning's friction coefficient for the channel is 0.03. The flow is supercritical at inflow, with depth $\hat{y}(0)$ and supercritical at outflow.

The exact solution for this problem is $y(x) \equiv \hat{y}(x)$.

Problem 3 *Transcritical Flow*

A rectangular channel, $0 \leq x \leq 100m$, has width $10m$ and a discharge of $20m^3s^{-1}$. The slope of the channel is given by

$$S_0(x) = \left(1 - \frac{4}{g[\hat{y}(x)]^3}\right) \hat{y}'(x) + \frac{9}{2500[\hat{y}(x)]^2} \left(\frac{1}{5} + \frac{1}{\hat{y}(x)}\right)^{4/3},$$

where

$$\hat{y}(x) = \left(\frac{4}{g}\right)^{1/3} \left(1 - \frac{(x-50)}{200} + \frac{(x-50)^2}{30000}\right),$$

and

$$\hat{y}'(x) = \left(\frac{4}{g}\right)^{1/3} \left(-\frac{1}{200} + \frac{(x-50)}{15000}\right).$$

Manning's friction coefficient for the channel is 0.03. The flow is subcritical at inflow and supercritical at outflow.

The exact solution for this problem is $y(x) \equiv \hat{y}(x)$.

Problem 4 Sub-Super-Subcritical Flow with Hydraulic Jump

A rectangular channel, $0 \leq x \leq 100m$, has width $10m$ and a discharge of $20m^3s^{-1}$. The slope of the channel is given by

$$S_0(x) = \left(1 - \frac{4}{g[\hat{y}(x)]^3}\right) \hat{y}'(x) + \frac{9}{2500[\hat{y}(x)]^2} \left(\frac{1}{5} + \frac{1}{\hat{y}(x)}\right)^{4/3},$$

where

$$\hat{y}(x) = \begin{cases} \left(\frac{4}{g}\right)^{1/3} \left(\frac{4}{3} - \frac{x}{100}\right) - \frac{9x}{1000} \left(\frac{x}{100} - \frac{2}{3}\right) & x \leq \frac{200}{3} \\ \left(\frac{4}{g}\right)^{1/3} \left(0.674202 \left(\frac{x}{100} - \frac{2}{3}\right)^4 + 0.674202 \left(\frac{x}{100} - \frac{2}{3}\right)^3 - 21.7112 \left(\frac{x}{100} - \frac{2}{3}\right)^2 + 14.492 \left(\frac{x}{100} - \frac{2}{3}\right) + 1.4305\right) & x > \frac{200}{3} \end{cases},$$

and

$$\hat{y}'(x) = \begin{cases} \frac{-1}{100} \left(\frac{4}{g}\right)^{1/3} - \frac{9}{500} \left(\frac{x}{100} - \frac{1}{3}\right) & x \leq \frac{200}{3} \\ \left(\frac{4}{g}\right)^{1/3} \left(0.02696808 \left(\frac{x}{100} - \frac{2}{3}\right)^3 + 0.02022606 \left(\frac{x}{100} - \frac{2}{3}\right)^2 - 0.434224 \left(\frac{x}{100} - \frac{2}{3}\right) + 0.14492\right) & x > \frac{200}{3} \end{cases}.$$

Manning's friction coefficient for the channel is 0.03. The flow is subcritical at outflow, with depth $\hat{y}(100)$, and subcritical at inflow.

The exact solution for this problem is $y(x) \equiv \hat{y}(x)$.

Problem 5 Sub-Super-Subcritical Flow with Hydraulic Jump

A rectangular channel, $0 \leq x \leq 100m$, has width $10m$ and a discharge of $20m^3s^{-1}$. The slope of the channel is given by

$$S_0(x) = \left(1 - \frac{4}{g[\hat{y}(x)]^3}\right) \hat{y}'(x) + \frac{9}{2500[\hat{y}(x)]^2} \left(\frac{1}{5} + \frac{1}{\hat{y}(x)}\right)^{4/3},$$

where

$$\hat{y}(x) = \begin{cases} \left(\frac{4}{g}\right)^{1/3} \left(-10.7872 \left(\frac{x}{100} - \frac{1}{3}\right)^4 + 18.8777 \left(\frac{x}{100} - \frac{1}{3}\right)^3 + 17.9329 \left(\frac{x}{100} - \frac{1}{3}\right)^2 + 3.1725 \left(\frac{x}{100} - \frac{1}{3}\right) + 0.850042\right) & x \leq \frac{100}{3} \\ \left(\frac{4}{g}\right)^{1/3} \left(\frac{5}{6} + \frac{(100-x)}{200}\right) + \frac{4}{10} \left(\frac{x}{100} - \frac{1}{3}\right) \left(\frac{x}{100} - 1\right) & x > \frac{100}{3} \end{cases},$$

and

$$\hat{y}'(x) = \begin{cases} \left(\frac{4}{g}\right)^{1/3} \left(-0.431488 \left(\frac{x}{100} - \frac{1}{3}\right)^3 + 0.566331 \left(\frac{x}{100} - \frac{1}{3}\right)^2 + 0.358658 \left(\frac{x}{100} - \frac{1}{3}\right) + 0.031725\right) & x \leq \frac{100}{3} \\ \frac{-1}{200} \left(\frac{4}{g}\right)^{1/3} + \frac{4}{500} \left(\frac{x}{100} - \frac{2}{3}\right) & x > \frac{100}{3} \end{cases} .$$

Manning's friction coefficient for the channel is 0.03. The flow is supercritical at inflow, with depth $\hat{y}(0)$ and supercritical at outflow.

The exact solution for this problem is $y(x) \equiv \hat{y}(x)$.